Rare Met. (2024) 43(10):4844–4866
https://doi.org/10.1007/s12598-024-02727-4

RARE METALS

REVIEW

Rational design and energy catalytic application of high-loading single-atom catalysts

Zi-Wei Deng, Yue Liu, Jie Lin*, Wen-Xing Chen*

Received: 29 August 2023 / Revised: 29 September 2023 / Accepted: 7 October 2023 / Published online: 8 June 2024

Abstract It is well known that single-atom catalysts (SACs) have become a hot topic in the field of catalysis due to their advantages such as 100% metal atom utilization efficiency, high catalytic activity and selectivity compared with conventional catalysts and nanocatalysts. However, the isolated metal atoms on SACs have thermodynamic instability and tend to agglomerate, which limit their catalytic performance. Therefore, it is of great significance to synthesize stable and high-loading single-atom catalysts (HLSACs). In this paper, we review the research progress of HLSACs from two aspects: design and application. Firstly, we comprehensively introduce the synthesis strategies of HLSACs, namely, top-down and bottom-up methods. Secondly, we overview the application status of HLSACs in three fields: electrocatalysis, thermal catalysis and photocatalysis. Finally, we summarize the development prospects and challenges of HLSACs.

Keywords High-loading single-atom catalysts; Design; Electrocatalysis; Thermal catalysis; Photocatalysis

1 Introduction

At present, the rapid development of industry has driven economic growth, improved overall living standards and promoted scientific and technological innovation and technological progress, but it has also brought some problems, such as environmental pollution and energy shortage. Catalysts have attracted much attention due to their application in the environment [1–3], energy [2, 4, 5], medicine [6, 7] and other fields. Firstly, they can be used to degrade organic pollutants and reduce harmful gas emissions [8]. Secondly, they can be used to produce clean and renewable energy [9], such as ethanol, hydrogen, etc. Additionally, they can optimize energy utilization efficiency, improve battery performance and stability, among other applications [10, 11]. Nowadays, there are two common types of catalysts: homogeneous and heterogeneous. Homogeneous catalysts have the advantages of fast reaction rate and easy control of reaction conditions, while heterogeneous catalysts have the benefits of simple separation and recovery and good stability [12]. However, there are some problems in the application of both types of catalysts. For example, acid–base catalysts, biological catalysts and other homogeneous catalysts are difficult to separate and recover due to their being in the same phase as the reactants, and their low stability; iron, zeolite, activated carbon and other heterogeneous catalysts have a slow reaction rate due to the diffusion resistance encountered when reacting with the reactants. Single-atom catalysts (SACs) that combine the advantages of homogeneous and heterogeneous catalysts have gradually become one of the focuses of researches [13, 14].

SACs are a type of catalysts in which metal atoms are dispersed on carriers without metal–metal bonds [15, 16]. They offer unique advantages over traditional nanocatalysts, including higher metal utilization rates, lower catalytic costs and improved electronic structures. The performance of SACs is influenced by factors such as the

Z.-W. Deng, W.-X. Chen*
Energy and Catalysis Center, School of Materials Science and Engineering, Beijing Institute of Technology, Beijing 100081, China
e-mail: wxchen@bit.edu.cn

Y. Liu, J. Lin*
Ningbo Institute of Materials Technology and Engineering, Chinese Academy of Science, Ningbo 315201, China
e-mail: linjie@nimte.ac.cn

number of active sites, defects, charge leakage and the interaction between the metal and support. The discovery and definition of SACs took more than a decade. As early as 1995, Thomas and co-workers found a catalyst with no visible nanoparticles, suggesting the presence of isolated Ti active sites [17]. However, limitations in technology at that time prevented confirmation at the atomic scale. It was not until 2011 that Zhang et al. confirmed the existence of SACs by preparing Pt_1/FeO_x for CO oxidation and observing isolated Pt atoms using high-angle annular dark-field scanning tunneling microscope (HAADF-STEM) and X-ray absorption fine structure analysis [18]. SACs, with their high atomic utilization rate, high reaction activity and good reaction selectivity, are a new type of supported catalyst with various types including precious and non-precious metals dispersed on carbon materials, porous materials, metals or non-metals. Different types of SACs with excellent catalytic performance have diverse applications in electrocatalysis, thermal catalysis and photocatalysis.

The catalytic performance of catalysts is directly related to the number of active catalytic sites. The greater the number of active sites, the higher the performance. However, most SACs have a low loading (less than 1 wt%) in order to ensure the dispersion of metal atoms, which limits their effectiveness in practical industrial applications. Therefore, one way to enhance catalytic performance is through the synthesis of HLSACs, which can increase the number of active sites. However, achieving high loading also presents challenges due to the tendency of metal atoms to aggregate, caused by their high surface energy and thermal instability. Consequently, the synthesis of HLSACs is a challenging task. Nowadays, significant progress has been made by scientists in achieving high loading of SACs. Figure 1 illustrates the representative advancements of HLSACs from 2016 to 2023. For instance, Yin et al. [19] employed a special pyrolysis strategy to prepare Co SACs with a loading of over 4 wt% on nitrogen-doped porous carbon, demonstrating better performance in oxygen reduction reaction (ORR) than most catalysts [20, 21]. Han and co-workers [22] used layered porous carbon as a support to synthesize Mo SACs for electrocatalytic nitrogen reduction (NRR), achieving a loading of up to 9.54 wt% and showcasing superior NRR performance [23–25]. Zhao et al. [26] reported a general strategy for large-scale production of M-NC SACs with metal loadings of up to 12.1 wt%. Of note, Fe-NC SAC and Ni-NC SAC exhibited excellent ORR and CO_2 reduction reaction (CO_2RR) performance, respectively. Xiong et al. [27] even achieved metal loading of up to 30 wt% in small batches, laying the foundation for potential industrial applications. Notably, SAS-Fe had excellent selectivity (89%) in styrene epoxidation, surpassing a Co SAC (71%) with a loading of 3.2 wt% reported by Bai et al. [28]. Besides, Wang et al. [29] utilized a carbon-based support prepared from graphene quantum dots to successfully synthesize high-density SACs with loadings of up to 40 wt% of transition metals. This carbon-based support contains multiple anchoring sites, maintaining appropriate distances between metal atoms and effectively preventing metal aggregation. While there have been numerious reviews on SACs in recent years, there is a dearth of the literature specifically focused on HLSACs. Most exciting reviews solely address individual aspects and fail to integrate the synthesis strategies and applications of HLSACs [30, 31].

In this review, we provide a comprehensive summary of the design strategies and energy catalysis applications of HLSACs (Fig. 2). The synthesis strategies discussed include both top-down and bottom-up approaches, with a focus on various preparation methods for achieving high-loading catalysts with a loading of more than 1 wt%, such as the wet chemical method, pyrolysis method, atomic layer deposition (ALD), electrochemical method and so on. Furthermore, we review the significant applications of HLSACs in electrocatalysis, photocatalysis and thermal catalysis, emphasizing their superior performance compared to homogeneous and heterogeneous catalysts. We firmly believe that HLSACs offer immense research potential, with the loading capacity capable of achieving greater breakthroughs, ultimately leading to even more excellent catalytic performance.

2 Synthesis strategies of HLSACs

After decades of development, SACs have made significant progress in synthesis, characterization and application. The synthesis strategies for SACs can generally be divided into top-down and bottom-up approaches. The top-down synthesis strategy involves starting with nanoparticles or larger elements (metals, oxides, etc.) as metal precursors and converting them into single atoms through pyrolysis or other conditions. This process breaks down the larger metal structures into individual atoms, thus achieving high dispersity. However, it is less commonly used for HLSACs synthesis. The bottom-up synthesis strategy is more commonly employed for HLSACs synthesis. In this approach, the metal precursor is adsorbed onto a carrier material and then anchored at defects or specific sites on the carrier through various reduction methods, resulting in the formation of SACs [37]. In recent years, significant progress has been made in the synthesis of HLSACs from both top-down and bottom-up perspectives. Here, we summarize some of the prominent methods for synthesizing HLSACs.

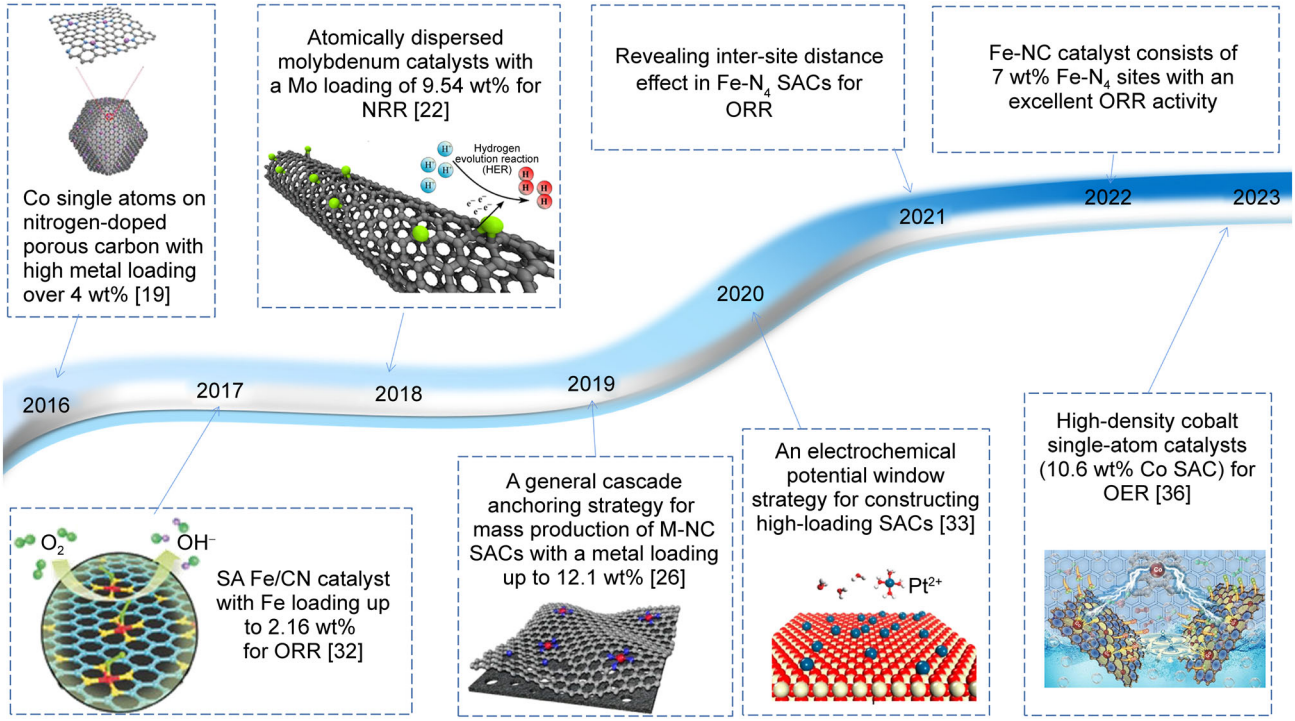

Fig. 1 Representative advances of HLSACs between 2016 and 2023 [19, 22, 26, 32–36]

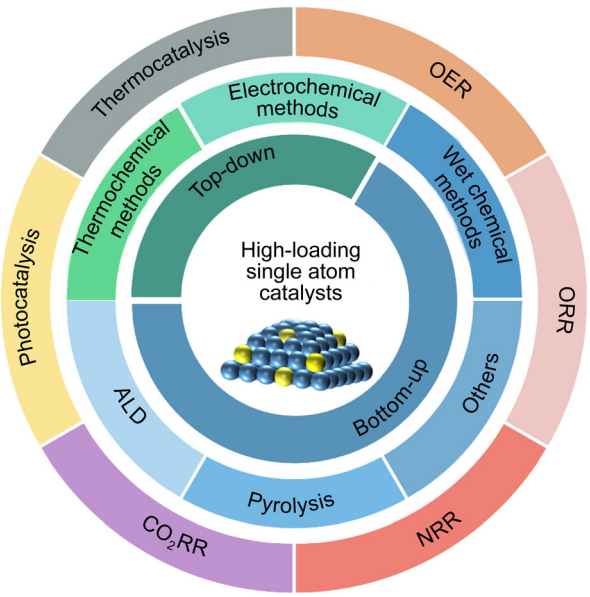

Fig. 2 Schematic diagram of HLSACs

2.1 Top-down strategies for HLSACs

According to the different energy sources used to promote the decomposition, replacement or reduction of metal precursors, the synthesis of HLSACs is divided into two parts: the thermal method and the electrochemical method.

2.1.1 Thermochemical methods

At present, important progress has been made in converting large-particle nanomaterials of metals or metal oxides into SACs by thermochemical methods. Jones et al. [38] used high temperature to decompose platinum (Pt) nanoparticles into single Pt atoms and firmly anchored them onto ceria nanorods. This approach not only prevented atom re-aggregation, but also enhanced the binding between atoms and the support, thereby improving the stability of SACs. Hence, this method is suitable for preparing HLSACs.

Among these methods, the confinement pyrolysis strategy is a thermochemical technique that effectively prevents atoms aggregation during the preparation of SACs. It consists of two steps: encapsulation and pyrolysis. Liu et al. [39] employed this strategy by initially encapsulating graphene nanosheets onto magnetite using a cross-linked polymer to create a confined structure. Subsequently, they pyrolyzed it at high temperature under an inert atmosphere, resulting in SA Fe/C with a loading of 13.7 wt% (Fig. 3a). The same method can also be used to prepare Co SACs, Ni SACs, Mn SACs and other with loadings over 10 wt%. SACs produced via this method exhibited high activity, high dispersion and high stability, although they have certain limitations regarding the choice of support.

Chemical vapor deposition (CVD) is a process that converts gaseous substances into solid deposits, occurring in the gas phase or at the gas–solid interface. It is one of the

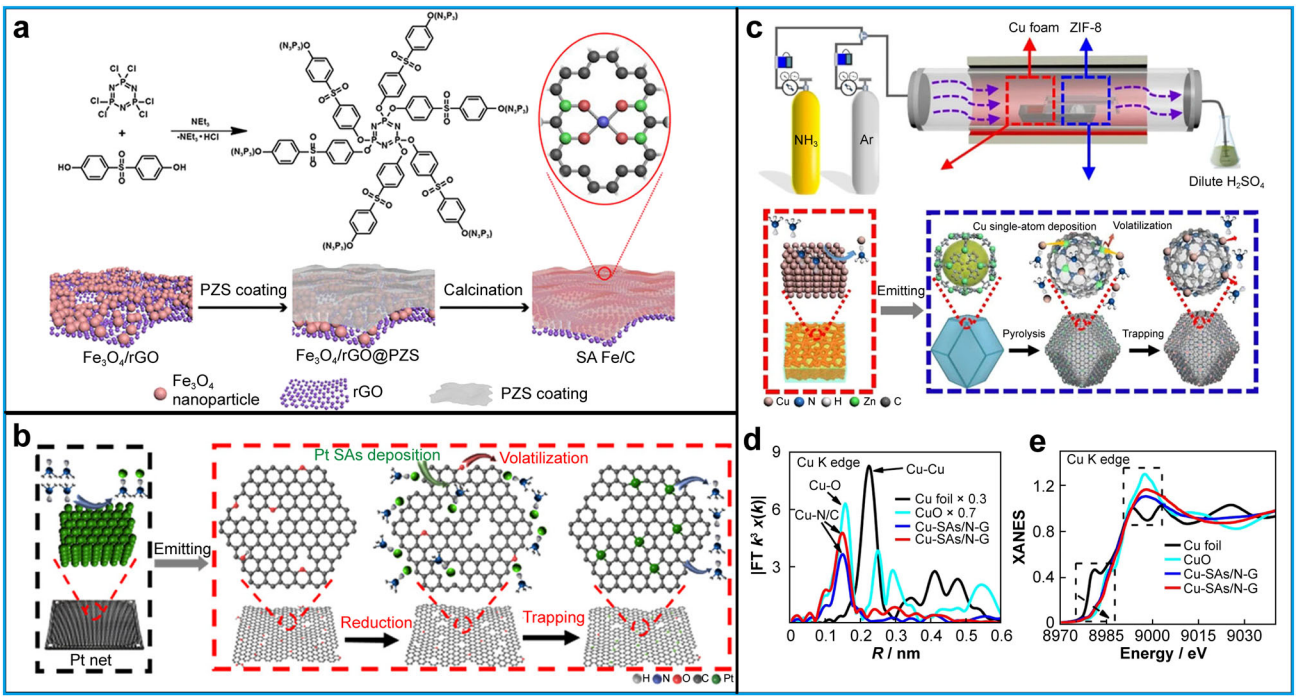

Fig. 3 Thermochemical methods for synthesizing HLSACs. **a** Synthetic process of SA Fe/C. Reproduced with permission from Ref. [39]. Copyright 2021, Wiley–VCH GmbH. **b** Reaction mechanism of Pt SAs/DG. Reproduced with permission from Ref. [42]. Copyright 2019, American Chemical Society. **c** Device diagram and reaction mechanism of Cu-SAs/N–C; **d** K^3-weighted χ(k) function of EXAFS spectra; **e** Cu K edge X-ray absorption near-edge structure (XANES) spectra. Reproduced with permission from Ref. [43]. Copyright 2018, Nature Publishing Group

general methods for preparing SACs. In the CVD process, the reactant gas first diffuses to the surface of the substrate, adsorbs and reacts on it, leading to the formation of solid deposits [40, 41]. Although CVD method has some disadvantages, such as strict application conditions, high-temperature and -pressure requirements and low efficiency, it can be employed to prepare HLSACs in top-down synthesis methods. For instance, Qu and colleagues [42] proposed a thermal emitting strategy to convert Pt nets into Pt atoms supported on defective graphene, as shown in Fig. 3b. Defective graphene was obtained by heat-treating graphene oxide at 1100 °C. Due to the strong coordination effect of ammonia gas generated by the thermal decomposition of dicyandiamide with Pt atoms, volatile $Pt(NH_3)_x$ can be formed and immobilized on the defective graphene surface, facilitating the loading process. Ultimately, a Pt SAs/DG catalyst with a loading of 2.1 wt% was obtained. Li and co-works developed a gas migration method to obtain Cu single atoms dispersed on nitrogen-doped carbon (Cu-SAs/N–C), with a loading of 1.26 wt % [43]. The reaction device and mechanism are depicted in Fig. 3c. Initially, zeolitic imidazolate framework-8 (ZIF-8) was pyrolyzed in an inert argon gas environment to generate a carrier material with abundant defect sites. Subsequently, ammonia gas was introduced to extract copper atoms from bulk copper foam, forming volatile $Cu(NH_3)_x$. Finally, $Cu(NH_3)_x$ was captured by the nitrogen-rich carbon carrier defects. Extended X-ray absorption fine structure (EXAFS) analysis (Fig. 3d) and X-ray absorption near-edge structure (XANES) spectrum (Fig. 3e) confirmed that the coordination environment of the catalysts involved one Cu atom with four nitrogen coordination to it. It is evident that ammonia gas plays a crucial role in the CVD-assisted synthesis method by selectively extracting metal atoms from the source at high temperature and immobilizing them onto the defects of the carrier.

2.1.2 Electrochemical methods

Electrochemical synthesis methods have been widely used in the preparation of nanocatalysts due to their advantages such as simplicity, mild reaction conditions, and easy control over catalyst morphology and composition (by controlling temperature, current, voltage, electrolyte, etc.). Various electrochemical techniques, including electrodeposition, cathodic corrosion, electrochemical dealloying, galvanic replacement, electrochemical exfoliation and electrochemical modification, have been employed for the synthesis of HLSACs [44]. Electrochemical methods can achieve the dispersion and stabilization of atoms by selecting relevant parameters, avoiding the reaggregation and loss of atoms. There have reports of using electrochemical methods to

prepare HLSACs. One example is the electrodeposition method used by Zhang and co-works [45] to prepare Pt SA-NT-NF catalyst with a loading of 1.76 wt% Pt atoms dispersed on the surface of CoP-based nanotube arrays NF. The synthesis process is illustrated in Fig. 4a. A three-electrode electrolytic cell was utilized, with a phosphate buffer solution as the electrolyte (pH = 7.2), Pt foil as the counter electrode, saturated calomel electrode as the reference electrode and the carrier of the SACs as the working electrode. After cycling the potential for 5000 times, the Pt SA-NT-NF catalyst was obtained. The hydrogen evolution reaction (HER) performance of the catalyst remained stable even after 7500 and 10,000 cycles (Fig. 4b). Aberration-corrected scanning tunneling electron microscopy (AC-TEM) images revealed that Pt was distributed on the carrier in the form of atomic dispersion (Fig. 4c, d). X-ray diffraction (XRD) (Fig. 4e) and X-ray photoelectron spectroscopy (XPS) (Fig. 4f) analyses demonstrated the absence of diffraction peaks corresponding to Pt crystals or Pt_0, indicating that Pt in Pt SA-NT-NF existed solely as single atoms without Pt grains. The resulting Pt SAC electrode exhibited a large area, binder-free characteristics and excellent performance, providing a feasible method for synthesizing Pt SAC electrodes with similar requirements and holding broad application prospects.

The dangling bond trapping strategy is a top-down approach that can be used to prepare high metal loading SACs, which is an effective means besides thermal and electrochemical methods. The strategy employs the use of dangling bonds on the surface of a carbon material carrier to trap metal atoms, which are then pulled out of the metal foam by ultrasonic waves, resulting in catalysts with single-atom sites. Qu et al. [46] used this strategy to transform bulk Fe metal foam into high-density SACs with a Fe loading of 6.7 wt% at room temperature. The synthesis method involved adjusting the oxygen–iron bonding at the interface between graphene oxide and metal foam. Specifically, they mixed graphene oxide slurry with Fe metal foam and dried it at room temperature. Due to the close contact between graphene oxide and iron, charge transfer occurred, generating abundant $Fe^{\delta+}$ $(0 < \delta < 3)$ species, which can form coordination bonds with dangling bonds. Finally, through ultrasonic waves, iron atoms were separated from the metal foam and formed Fe SAs/GO. This strategy exhibits broad applicability, a simple preparation process, and holds promising applications in industry.

2.2 Bottom-up strategies for HLSACs

Bottom-up synthesis strategies have been widely used in HLSACs, including impregnation, coprecipitation, chemical vapor deposition, atomic layer deposition, etc.

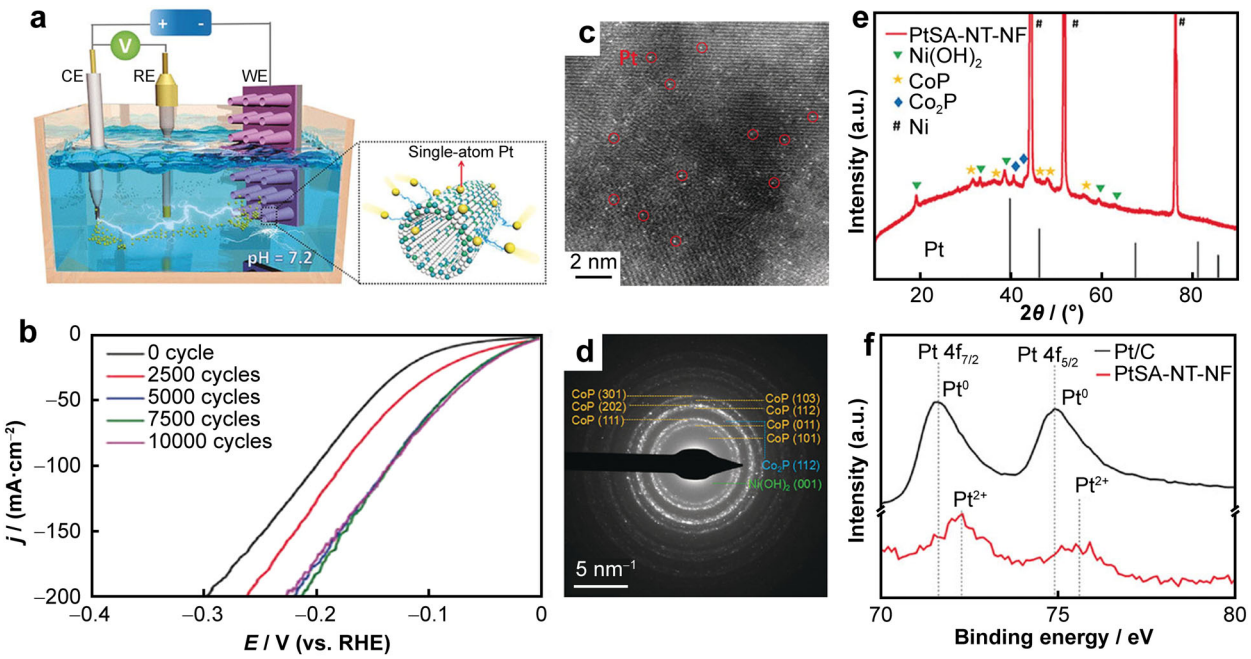

Fig. 4 Electrochemical methods for synthesizing HLSACs: **a** synthetic process of Pt SA-NT-NF; **b** HER polarization curves after performing different cycles on surface coming with CoP-based nanorods or nanoarrays NF; **c** AR HAADF image of Pt SA-NT-NF; **d** electron diffraction diagram of NTs; **e** XRD pattern of Pt SA-NT-NF and **f** XPS spectra of Pt SA-NT-NF and commercial 20 wt% Pt/C. Reproduced with permission from Ref. [45]. Copyright 2017, Wiley–VCH GmbH

2.2.1 Wet chemical methods

The wet chemical method is a technique that uses liquid solution to treat solid materials, allowing for various purposes such as etching and preparation [47]. In the preparation of SACs, wet chemical method is one of the earliest and most commonly used methods, which includes co-precipitation, impregnation and ion exchange, among others. This method mainly forms isolated metal sites on the surface of the carrier through sequential steps such as precipitation, reduction, activation and more. And it is simple to operate and enables the mass production and scale-up preparation of catalysts. Additionally, the metal loading and dispersion of SACs can be adjusted by changing the conditions within the solution.

In recent years, the wet chemical method has been widely used by researchers for the preparation of HLSACs. These methods have demonstrated universality and applicability to various metals, enabling kilogram-level production. For example, Hai et al. [48] proposed a general method that combined impregnation and two-step annealing. They successfully synthesized 15 different HLSACs with various metals, achieving a maximum loading of up to 23 wt%. The preparation process is shown in Fig. 5a. Firstly, the metal precursor was loaded on the carrier as much as possible. Then, the first annealing step was performed at a temperature lower than the decomposition temperature of the metal precursor. This step aims to remove some ligands, prevents nanoparticles formation and maintains the desired properties. Subsequently, the unanchored metal was washed away, followed by a second annealing to completely eliminate the remaining ligands, resulting in the formation of HLSACs. To illustrate the formation process of the catalysts, the authors analyzed the crucial species involved using techniques such as EXAFS (Fig. 5f) and XPS (Fig. 5g). In addition, they employed density functional theory (DFT) calculations (Fig. 5h) based on the determined atomic structure to demonstrate that the catalysts formation involved two endothermic and one spontaneous process. This further validates the necessity of using two-step annealing approach. Moreover, Kunwar et al. [49] prepared a single-atom Pt catalyst (Pt/CeO_2) by impregnating 3 wt% Pt onto a high surface area commercial ceria support. The catalyst exhibited exceptional thermal stability as the CeO_2 support prevented Pt atoms from clustering. When the Pt atoms were oxidized to PtO_2, they formed stable interactions with the Ce^{3+} reduced from CeO_2.

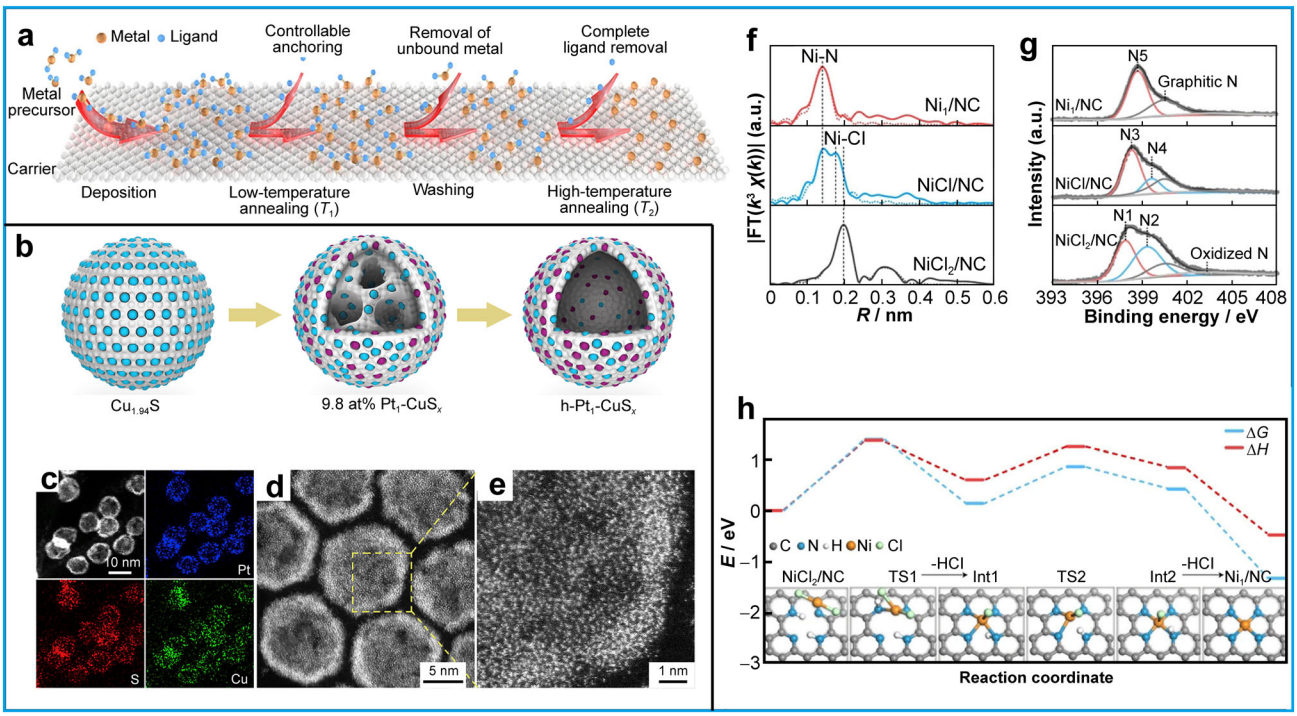

Fig. 5 Wet chemical methods for synthesizing HLSACs. **a** Strategy for preparing UHD-SACs; **f** Fourier-transformed EXAFS and **g** N 1s XPS spectra of $NiCl_2$/NC, NiCl/NC and Ni_1/NC and **h** DFT calculation of representative intermediates and transition states during the formation of $NiCl_2$ to Ni-N_4. Reproduced with permission from Ref. [48]. Copyright 2021, Nature Publishing Group. **b** Schematic diagram of structural changes of h-Pt_1-CuS_x during synthesis, where white ball represents S, blue ball represents Cu and purple ball represents Pt; **c** EDS spectra of Pt, S and Cu elements in h-Pt_1-CuS_x nanoparticles and **d**, **e** AC-HAADF-STEM images of h-Pt_1-CuS_x. Reproduced with permission from Ref. [50]. Copyright 2019, Elsevier Inc

The ion exchange method is another method used for the preparation of HLSACs. This method involves utilizing ion exchange resin as a carrier, where a metal precursor solution is mixed with the resin. The metal is loaded onto the resin, and SACs are obtained by decomposing the metal precursors into single atoms through annealing after undergoing washing, drying and other necessary steps. Zhang's group, for example, utilized iron-based ion exchange resin as a carrier to obtain Pt_1/FeO_x SACs [18]. This method allows for the achievement of uniform distribution and high dispersion of metals. Moreover, the metal loading and dispersion can be adjusted by controlling the conditions, making it suitable for the preparation of HLSACs.

In another study, Shen et al. [50] employed the ion exchange method to prepare SACs with a high Pt metal loading of 24.8 wt% (h-Pt_1-CuS_x), using hollow CuS_x as the carrier. The structural changes occurring during the catalyst preparation process are illustrated in Fig. 5b. Through energy-dispersive X-ray spectroscopy (EDS) mapping, it could be observed that the Pt, S and Cu elements were uniformly distributed in h-Pt_1-CuS_x (Fig. 5c). The catalyst exhibited a hollow structure (Fig. 5d), and Pt atoms were abundantly present on the surface of the carrier in an isolated state, as observed through AC-HAADF-STEM imaging (Fig. 5e).

2.2.2 Atomic layer deposition (ALD)

ALD is a chemical vapor deposition method that enables the production of dense, uniform and high-quality films. It operates by utilizing alternating pulses of different precursor chemicals and inert gas purge processes, allowing for precise control over the thickness and composition of deposited single atoms and nanoclusters [51, 52]. Compared to other deposition methods such as chemical vapor deposition (CVD) and physical vapor deposition (PVD), ALD offers several advantages in the synthesis of single-atoms synthesis process. ALD can effectively prevent atom aggregation, defects and other issues that may arise during the synthesis of single atoms. This method enables precise control over the position and number of metal atoms, leading to highly controllable and reproducible results.

The use of ALD in the preparation of SACs has demonstrated promising results. Sun et al. [53] were pioneers in applying the ALD method to load Pt atoms onto graphene nanosheets, resulting in SACs with excellent catalytic activity. Researchers have further advanced the ALD process to prepare HLSACs. For instance, Yan et al. [54] utilized graphene as the carrier and precisely controlled the density of Co single atoms loaded on it by adjusting the number of ALD cycles, achieving a loading of 2.5 wt%. To optimize the ALD process, they incorporated O_3 treatment during the cycle process (Fig. 6a). By oxidizing graphene at high temperature, uniform epoxy functional groups were generated, providing anchoring points to enhance Co loading. Simultaneously, this treatment removed the ligands from the precursor. As the number of ALD cycle increased, the Co loading also increased (Fig. 6c). However, even at a loading as high as 2.5 wt%, Co still remained in an atomically dispersed form. To investigate the local chemical environment of Co atoms, electron energy loss spectroscopy (EELS) measurement was conducted. These measurements revealed that oxygen atoms acted as anchors for the Co single atoms on graphene, confirming the presence of Co–O bonds (Fig. 6d). X-ray absorption fine structure spectroscopy (XAFS) (Fig. 6b) was used to analyze Co_1/G SACs with different loadings, and results indicated that Co was in an oxidized state. The atomic structure of Co_1/G SACs was elucidated through DFT calculations and other techniques. It was found that SACs consisted of a single cobalt atom coordinated with two interface oxygen atoms and four carbon atoms. These findings provide valuable insights into the atomic structure and coordination environment of Co in graphene-based SACs.

2.2.3 Pyrolysis

Pyrolysis is a widely used method for preparing SACs. The process involves coordinating metal precursors with carbon-based materials or metal–organic framework materials, as well as other supports. Metal atoms are then anchored on the surface of the support and subjected to pyrolysis in a high-temperature inert atmosphere. This transformation converts the metal precursors into single atoms while removing organic ligands and impurities, resulting in the formation of SACs. The method is known for its simplicity, efficiency, low cost and suitability for mass production. It also offers versatility and tunability, allowing the preparation of various types of SACs with different properties. Additionally, pyrolysis enables the production of SACs with high-loading and high-dispersion capabilities.

Pyrolysis is also commonly employed in the synthesis of high-loading transition metal SACs. For example, Wei et al. [55] used the "pre-adsorption-anchoring-pyrolysis" method to prepare Zn-N_3O SACs with a loading capacity of up to 11.34 wt%. These SACs exhibited an asymmetric coordination structure of Zn-N_3O active sites. The synthesis process is illustrated in Fig. 7d. Initially, polypyrrole (PPy) nanowires were prepared through an improved chemical oxidative polymerization method. Subsequently, PPy was mixed and dried with $Zn(NO_3)_2{\cdot}6H_2O$ and 2-methylimidazole to obtain Z-PPy. Finally, Z-PPy was

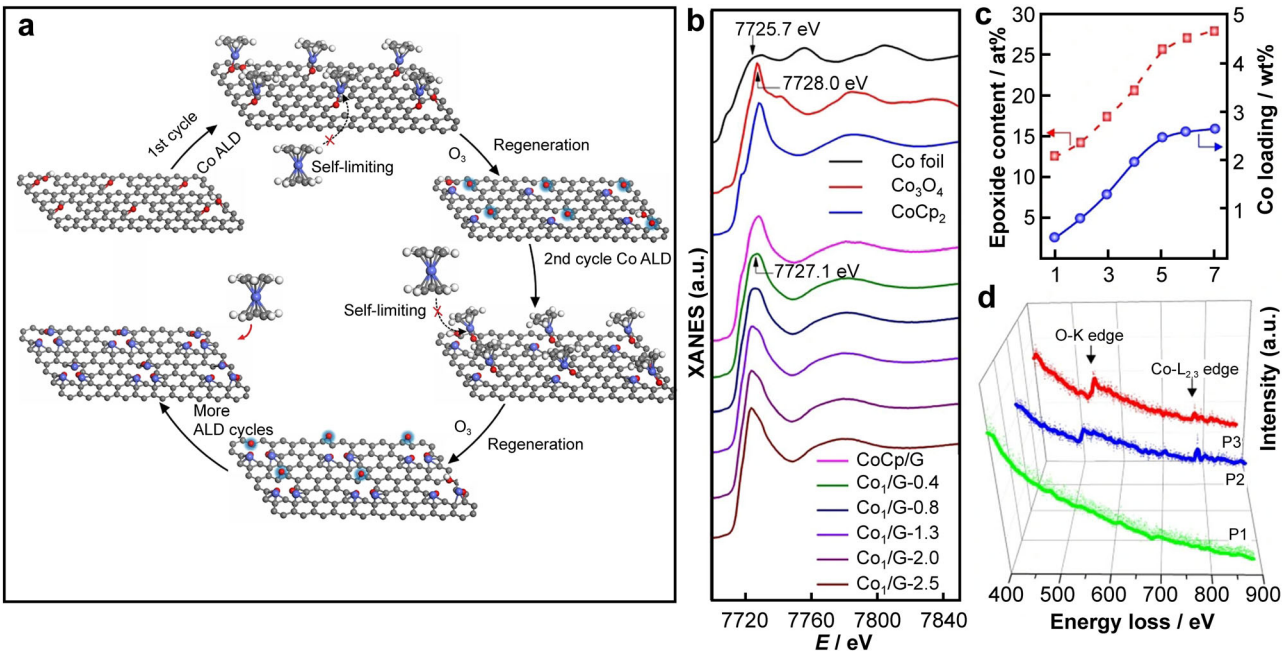

Fig. 6 ALD for synthesizing HLSACs: **a** synthetic process of Co_1/G SACs; **b** Co K-edge XAFS spectra; **c** as the number of ALD cycles increases, epoxy content in graphene and Co loading in Co_1/G SACs catalyst change and **d** EEL spectra of O K-edge and Co $L_{2,3}$-edge obtained in three different regions of bare graphene (P1, P2 and P3). Reproduced with permission from Ref. [54]. Copyright 2018, Nature Publishing Group

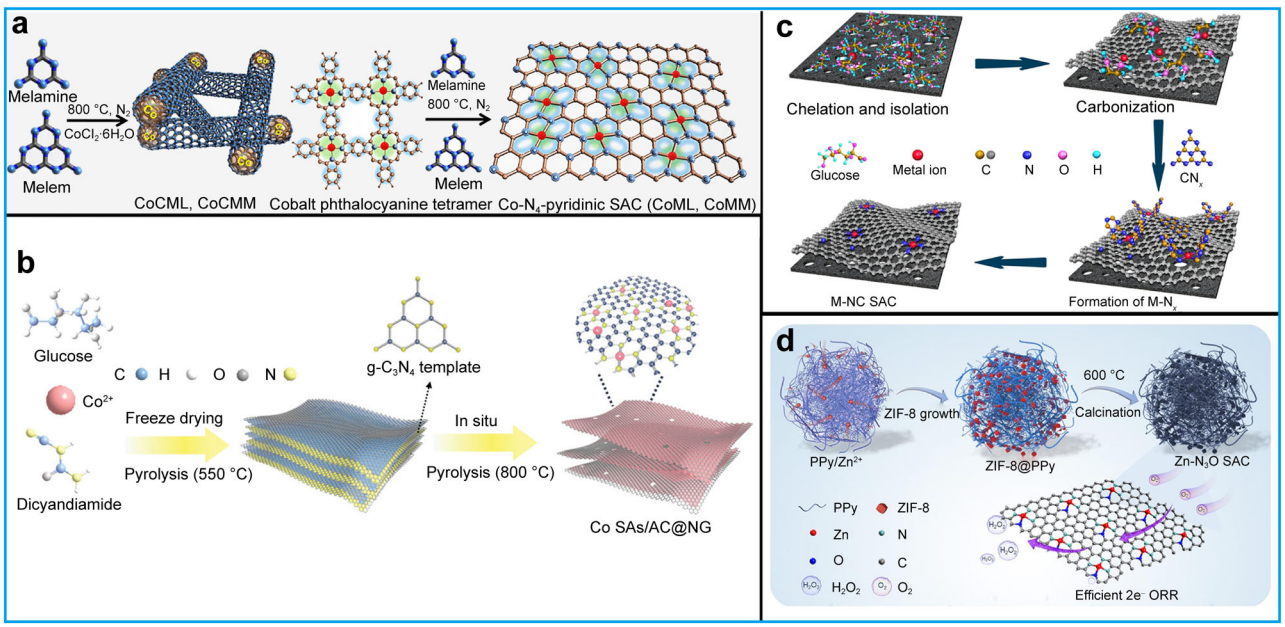

Fig. 7 Pyrolysis for synthesizing HLSACs. **a** Synthetic process of CoCML (materials prepared using melamine), CoCMM (materials prepared using melem) and Co-N_4-pyridinic SACs. Reproduced with permission from Ref. [36]. Copyright 2023, American Chemical Society. **b** Synthetic process of Co SAs/AC@NG. Reproduced with permission from Ref. [56]. Copyright 2022 Wiley–VCH GmbH. **c** Synthetic process of M-NC SACs. Reproduced with permission from Ref. [26]. Copyright 2019, Nature Publishing Group. **d** Synthetic process of Zn-N_3O SAC. Reproduced with permission from Ref. [55]. Copyright 2022, Elsevier B.V

calcined at 600 °C for 3 h under an inert atmosphere, followed by acid-washing, water-washing and drying to obtain Zn-N_3O SAC. Similarly, Mehmood et al. and Zhao et al. achieved the synthesis of high-loading Fe-NC SACs with loadings of 7 wt% and 12.1 wt% by pyrolysis. In their approach, Mehmood et al. [35] pyrolyzed ZIF-8 at 900 °C

in an N_2 atmosphere to obtain Zn-NC containing a large number of Zn-N_x sites. They then etched away Zn using acid, refluxed in ferric chloride for ion exchange to obtain Fe–N and finally activated it at high temperature to obtain Fe-NC SAC. However, the scalability of this method is somewhat limited due to the acid etching process. Zhao et al. [26] used a cascade anchoring strategy to produce high-loading single atoms. Glucose was used as a chelating agent, playing a dual protective role in the synthesis process of the catalyst (Fig. 7c). First, glucose chelated with the metal ions, effectively isolating them. Secondly, excess glucose bound to the surface of a nitrogen-rich porous carbon carrier, physically isolating the metal complexes. The metal ions and chelating agent were then mixed with melamine and subjected to pyrolysis, isolating the metal complexes. The metal ions and chelating agent were then mixed with melamine and subjected to pyrolysis, resulting in the formation of Fe-NC SACs. In this preparation process, high-temperature pyrolysis is necessary. Therefore, the stability of high-loading single atoms strongly depends on the strong binding force between the Fe single atoms and N atoms. This method can also be applied to prepare other high-loading SACs such as Mn, Co, Mo, Cu, etc. Kumar et al. and Zhang et al. also utilized pyrolysis to prepare high-loading Co SACs using nitrogen-doped carbon as the carrier. Among them, Kumar et al. [36] employed a macromolecule-assisted strategy to synthesize high-density Co single-atom sites in a pyridine-rich n-graphite network. They used CoPc and melem monomers, as depicted in Fig. 7a. Zhang et al. [56] employed a self-sacrificial template strategy to obtain Co SAs/AC@NG. The graphitic carbon nitride template was obtained through the pyrolysis of dicyandiamide, which provided abundant anchoring sites capable of effectively capturing Co single atoms and clusters (Fig. 7b). Both methods successfully prepared Co SACs with loadings exceeding 10 wt%.

2.2.4 Other methods

In the bottom-up strategies for the preparation of HLSACs, in addition to the wet chemistry, ALD and pyrolysis methods described above, we will introduce other methods in this section. The laser planting strategy is indeed a novel and innovative method for preparing SACs. It utilizes laser pulses to create defects on various substrates, decompose metal precursors into metal atoms and fix them onto the substrate to form high-loading single atoms. This approach offers several advantages such as being mild, environmentally friendly, universal, portable, precise and efficient. One key advantage of the laser planting strategy is that it does not require the use of chemical reagents or high temperatures, making it a versatile method suitable for various metals and substrates. By adjusting the laser parameters, precise control over the deposition of single atoms can be achieved. Furthermore, this method can achieve high loadings of single atoms, surpassing what other methods can achieve. Researchers, as example by Wang and co-workers [57], have successfully used this method to prepare Pt SACs with a loading of up to 41.8 wt% on graphene quantum dots (GQDs). In their study, the sample underwent instantaneous and nanosecond-long heating during the preparation process, followed by rapid quenching in liquid hexane. The result (Fig. 8a) demonstrates that different laser frequencies lead to varying morphologies of metal deposition, specifically single atoms at high frequency, clusters at medium frequency and nanoparticles at low frequency. The effectiveness of the laser planting method in preventing atom aggregation and migration lies in its ability to create vacancy defects on the substrate surface using laser pulses, thus anchoring single atoms. This method exhibits broad applicability, and researchers have proposed a rule for designing high catalytically active catalysts based on theoretical and experimental studies. The rule suggests that the closer the distribution of each metal atom in the catalyst aligns with the distribution of the corresponding metal catalytic performance in the electrocatalytic volcano diagram, the better performance of the catalyst. Overall, the laser planting strategy offers a promising and versatile approach for preparing SACs with high loadings of single atoms. It combines the advantages of being environmentally friendly, efficient and capable of precise control, making it an exciting avenue for catalyst design and development.

One of the keys to obtaining SACs with high metal loading but no metal atoms aggregation is to find suitable carriers that provide enough anchoring points for the atoms. Metal–organic frameworks (MOFs) are porous crystalline materials obtained by coordinating metals or metal clusters with organic ligands [58]. The morphology and structure of MOFs can be tuned by selecting different metal centers and organic ligands. It can be divided into MOFs with a similar zeolite pore structure, namely, ZIF-8; MOFs with a high specific surface area and pore volume, namely, leviathan framework materials (MILs); MOFs with a topological structure, namely, network metal and organic framework materials (IRMOFs) and MOFs with a pore type structure and three-dimensional (3D) orthogonal channels, namely, pore-channel type framework materials (PCNs). MOFs with high specific surface area and easy functionalization are important supports and sacrificial precursor templates for preparing HLSACs [59]. Most previous studies have focused on bulk MOFs. For example, Li et al. [19] synthesized Co Sas/N–C by in situ pyrolysis of MOF (zeolite-like structure). Zuo et al. [60] reported a new surfactant-stabilized coordination strategy that loaded

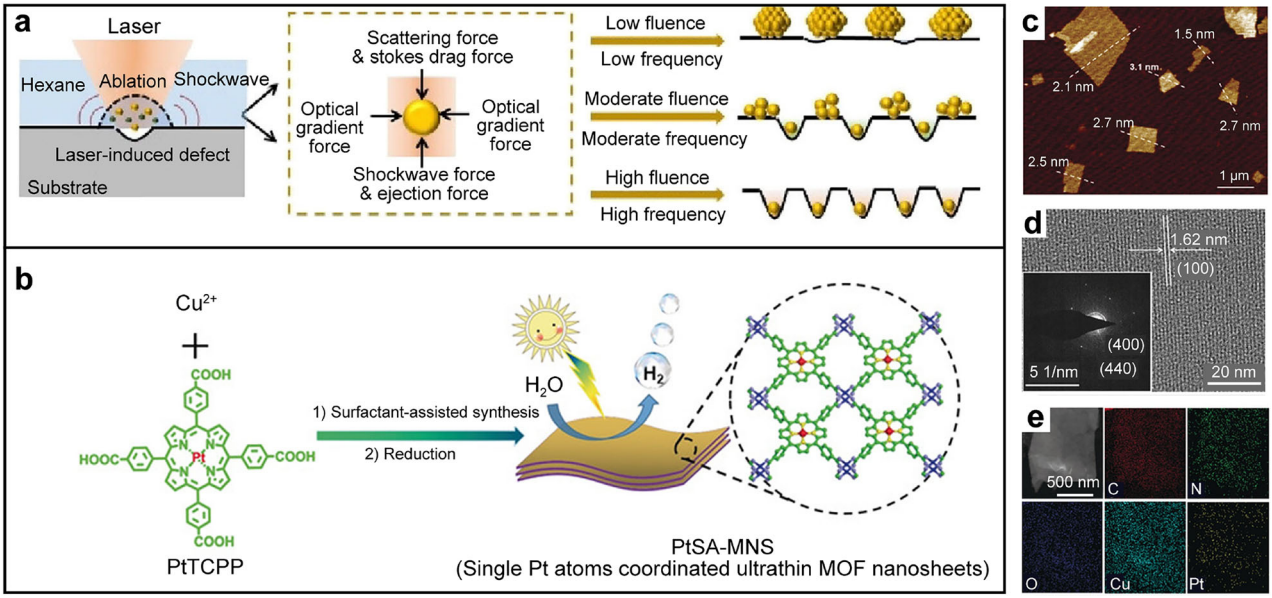

Fig. 8 Others methods for synthesizing HLSACs. **a** Synthesis process of Pt NPs, clusters and SAs under low-, medium- and high-frequency laser planting, respectively. Reproduced with permission from Ref. [57]. Copyright 2023, American Chemical Society. **b** Synthesis process of PtSA-MNSs for photocatalytic hydrogen production; **c** AFM height profile of PtSA-MNSs; **d** HRTEM image of PtSA-MNSs and (inset) SAED pattern and **e** elemental mapping images of PtSA-MNSs. Reproduced with permission from Ref. [60]. Copyright 2023, American Chemical Society

a high concentration of Pt atoms onto the ultra-thin two-dimensional (D) MOF nanosheets, resulting in Pt SA-MNSs with a loading of 12.0 wt%. The schematic diagram of the synthesis is shown in Fig. 8b, which is different from many SACs preparation methods in that Pt atoms are coordinated before the formation of MOF. The authors used $Cu_2(COO)_4$ as the metal center and PtII tetra(4-carboxyphenyl) porphyrin (Pt TCPP) as the organic ligand to synthesize 2D MOF with a large number of active sites, and finally obtained Pt SA-MNSs. The carrier was observed to be sheet-like and almost transparent by transmission electron microscopy (TEM), and the thickness of the nanosheets was about 2.4 nm by atomic force microscopy (AFM) analysis (Fig. 8c), indicating that the synthesized MOF was ultra-thin sheet-like. The lattice stripes on the MOF observed by high-resolution transmission electron microscopy (HRTEM) (Fig. 8d) were consistent with XRD analysis results, proving that it was crystalline. And EDS analysis (Fig. 8e) showed that C, N, O, Cu and Pt were evenly distributed on the catalyst.

3 Application of HLSACs

HLSACs, with their high metal utilization, multiple active sites and high catalytic activity, find wide-ranging applications in fields such as batteries, environment production and the chemical industry. In this section, we will elaborate on the application of HLSACs in electrocatalysis, thermal catalysis and photocatalysis.

3.1 Electrocatalysis

Electrocatalysis is a process that uses electricity to drive chemical reactions, enabling sustainable energy utilization and the preparation of high-value-added products. In electrocatalytic reactions, CO_2, H_2O, N_2, O_2 and other raw materials can be converted into fuels and value-added chemicals, such as methanol, ammonia, ethanol, acetic acid, etc. The efficiency of electrocatalysis is affected by various factors, including the quality of the electrode materials, the composition of the electrolyte solutions, the nature of the catalysts and parameters related to the electrochemical structure of reactor, current density and stirring speed. The catalyst, among these factors, is a key component that plays a critical role in improving reaction efficiency and stability.

3.1.1 Oxygen reduction reaction (ORR)

ORR is a process where oxygen gas is reduced to water or hydrogen peroxide on the surface of an electrode. The mechanism and pathways of ORR differ in alkaline and acidic environments [61, 62]. In alkaline environment, ORR can proceed through four-electron or two-electron ways. The reaction equation for the four-electron pathway is: $O_2 + 2H_2O + 4e^- \rightarrow 4OH^-$; the reaction equation for

the two-electron pathway is: $O_2 + 2H_2O + 2e^- \rightarrow 2H_2O_2$. In an acidic environment, ORR only follows the four-electron pathway, and the reaction equation is: $O_2 + 4H^+ + 4e^- \rightarrow 2H_2O$. The three key intermediates in ORR are *O, *OOH and *OH, which play different roles in the two-electron and four-electron pathways. In the two-electron pathway, the catalyst should have a moderate adsorption strength for *OOH. In the four-electron pathway, the ratio of the three intermediates affects the reaction rate, and the rate-determining step changes with the adsorption strength of the catalyst for these intermediates. If the catalyst has a strong adsorption for *OH, then *OH reduction becomes the rate-determining step; if the catalyst has a weak adsorption for *OH, then O_2 activation or O_2 reduction to form *OOH becomes the rate-determining step [63]. The reaction mechanism can be classified into dissociation and association types. Due to its ability to convert chemical energy into electrical energy and its pollution-free reaction products, ORR holds significant application value in the fields of fuel cells, metal–air batteries and electrochemical synthesis. In recent years, remarkable progress has been made in the research on high-loading single-atom electrocatalysis of ORR [64–66].

Metal–air batteries are a type of fuel cell that generates electricity through the oxidation–reduction reaction between metal and oxygen. This includes various types such as aluminum–air batteries, magnesium–air batteries, zinc–air batteries and lithium–air batteries. Among them, zinc–air batteries have gained attention due to their high-energy density, low cost and stability. Zhang et al. [56] reported a Co_{40} SAs/AC@NG catalyst for zinc–air batteries. This catalyst consists of porous nitrogen-doped graphene as the carrier, with a large number of Co single atoms and a small number of Co clusters loaded on the surface, achieving a loading of up to 14.0 wt%. The catalyst exhibited excellent kinetic for the ORR in an alkaline environment. It had a half-wave potential ($E_{1/2}$) of 0.890 V, a kinetic current density (J_k) of 27.64 $mA \cdot cm^{-2}$ (Fig. 9e) and a Tafel slope of 90 $mV \cdot dec^{-1}$ (Fig. 9e, f). The authors analyzed the high ORR activity of the catalyst using DFT calculation and found that it was attributed to both the Co single-atom sites and the Co AC/NC sites (Fig. 9g). Additionally, the catalyst demonstrated a high-energy density of up to 221 $mW \cdot cm^{-2}$ in zinc–air batteries. In contrast, Zhou et al. [67] prepared a Fe-SACs supported by N, S and fluorine (F) -co-doped porous graphitized carbon (Fe-SA-NSFC) catalyst with a higher loading amount (15.3 wt%) and better stability (Fig. 9b). The catalyst achieved a maximum power density of 247.7 $mW \cdot cm^{-2}$ in zinc–air electrode (Fig. 9a). Figure 9c shows the four-electron ORR process of the catalyst in alkaline environment. The catalyst utilizes NSFC as the carrier and enhances the thermodynamic driving force of ORR through S and F doping, as demonstrated by the free energy diagram (Fig. 9d). Compared with N-doped carbon (NC) and S- and N-co-doped carbon (NSC), the catalyst after S, F doping exhibits more favorable conditions for ORR.

Fuel cells are electrochemical devices that directly convert the chemical energy of a fuel into electrical energy, providing benefits such as high efficiency and low pollution. There are various types of fuel cells, including proton exchange membrane fuel cells (PEMFC), solid oxide fuel cells (SOFC) and anion exchange membrane fuel cells (AEMFCs). In fuel cells, efficient catalysts play a key role in promoting the ORR. Fe–N–C SACs are non-precious metal catalysts known for their good ORR activity. However, they are often poisoned by H_2O_2 generated during the reaction process, preventing ORR from being a complete $4e^-$ process. To address this challenge, Cao et al. [68] developed a Fe–Mn–N–C dual-atom catalyst (DACs) by pyrolysis method. This catalyst featured a FeN_4-MnN_3 dual-site structure on its surface with Fe and Mn content of 2.8 wt% and 1.46 wt%, respectively. Mechanism calculations by the authors showed that the Fe–Mn dual-site effectively suppressed $2e^-$ ORR and promoted $4e^-$ ORR by adsorbing oxygen in *OOH. Based on this catalyst, both PEMFC and AEMFCs showed excellent performance, achieving peak power densities of 1.048 and 1.321 $W \cdot cm^{-2}$, respectively.

3.1.2 Nitrogen reduction reaction (NRR)

Electrocatalytic nitrogen reduction is the process of converting nitrogen and water into ammonia using electricity. It offers a green and environmentally friendly approach to ammonia synthesis. The reaction pathways for electrocatalytic nitrogen reduction differ in alkaline and acidic environments. In alkaline environment, the pathway is: $N_2 + 6H_2O + 6e^- \rightarrow 2NH_3 + 6OH^-$; while in acidic conditions, it is: $N_2 + 6H^+ + 6e^- \rightarrow 2NH_3$. However, electrocatalytic nitrogen reduction faces challenges such as the inertness of N_2, high activation potential barrier, low solubility and competition from the hydrogen evolution reaction (HER). SACs have emerged as promising candidates for improving the kinetics of the nitrogen reduction reaction due to their unique advantages [69, 70].

HLSACs with carbon materials as carriers have shown excellent performance in electrocatalytic NRR. For example, Rh SA/GDY, Ru SA/GDY and Co SA/GDY with loading amounts of noble metals ranging from 12.08 wt% to 15.31 wt% were prepared and applied to NRR [71]. Rh SA/GDY effectively suppressed HER and enhanced NRR activity, achieving a high NH_3 production rate of 74.15 $\mu g \cdot h^{-1} \cdot cm^{-2}$ under pressurized conditions. Non-noble metal HLSACs have also been explored for NRR. Zang et al. [72] developed a Cu SAC with atomic dispersion, with a loading of 5.31 wt%. Cu SAC loading on porous

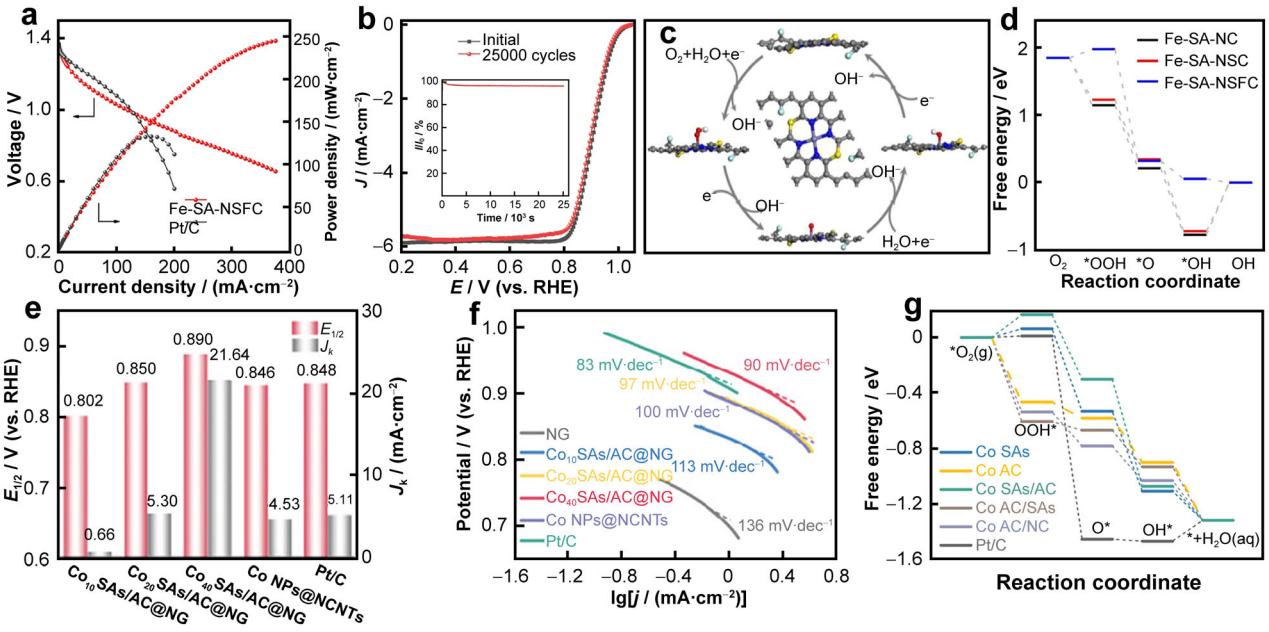

Fig. 9 ORR performance of HLSACs. **a** Discharge polarization curves and corresponding power density plots of Fe-SA-NSFC and Pt/C catalysts; **b** cyclic stability curve of Fe-SA-NSFC and its polarization curve before and after cycling; **c** $4e^-$ reduction mechanism of ORR for Fe-SA-NSFC catalyst in alkaline solution and **d** at a voltage of 0 V versus RHE, pH = 13, free energy diagram of Fe-SA-NC, FeSA-NSC and Fe-SA-NSFC. Reproduced with permission from Ref. [67]. Copyright 2020, Nature Publishing Group. **e** J_k at 0.85 V and $E_{1/2}$ for a range of samples; **f** Tafel curve of a series of samples at 0.1 mol·L^{-1} KOH and **g** free energy diagram of a series of samples. Reproduced with permission from Ref. [56]. Copyright 2022, Wiley–VCH GmbH

carbon materials, demonstrated pH universality and continuous operation for 12 h. The NH_3 production rates were 53.3 $\mu g_{NH3} \cdot h^{-1} \cdot mg_{cat}^{-1}$ in alkaline conditions and 49.3 $\mu g_{NH3} \cdot h^{-1}$ mg_{cat}^{-1} in acidic conditions. Mo single atoms anchored on nitrogen-doped porous carbon (SA-Mo/NPC) exhibited high Faraday efficiency of 14.6% ± 1.6% and high NH_3 yield of (34.0 ± 3.6) $\mu g_{NH3} \cdot h^{-1} \cdot mg_{cat}^{-1}$ when used for NRR [22]. Regarding the reaction mechanism of NRR, researchers have investigated various catalysts. For example, Fe_1/VS_2 catalyst with a Fe coverage of 11.1% demonstrated different hydrogenation pathways: distal, alternating and enzymatic [73]. By conducting DFT calculations, a hybrid mechanism called the distal–alternating mechanism was proposed based on the distal–enzymatic reaction pathway (Fig. 10a–d). This mechanism exhibited a low overpotential of only 0.35 V.

3.1.3 CO_2 reduction reaction (CO_2RR)

CO_2RR refers to the process of converting CO_2 into single-carbon (CO, CH_3OH) [74–76] or multi-carbon (CH_3CH_2OH, CH_3COOH, C_2H_4) chemicals and fuels [77–79] under the action of electricity. This process can reduce the pressure of carbon emissions and has wide applications in industry and energy [80, 81]. The products of CO_2RR are diverse, and here are some common equations of carbon dioxide reduction reactions: (1) $CO_2 + e^- \rightarrow CO + OH^-$; (2) $CO_2 + H^+ + e^- \rightarrow HCOOH$; (3) $CO_2 + 6H^+ + 6e^- \rightarrow CH_3OH + H_2O$ and (4) $2CO_2 + 12H^+ + 12e^- \rightarrow C_2H_4 + 4H_2O$. Different reduction products have different energy requirements, so we need to find electrocatalysts for CO_2RR that have high efficiency, selectivity, stability and performance.

HLSACs have great potential for improving the activity and selectivity of electrocatalytic reduction of CO_2. Currently, Ni SACs, as inexpensive and tunable SAC, can activate CO_2 and exhibit excellent CO_2RR performance with respect to CO. This has been widely studied. For example, Hai et al. [48] prepared Ni_1/NC through a two-step annealing method. This catalyst could electrocatalytically reduce CO_2 to CO. The catalyst had a particularly high loading, with a Ni loading amount of 16.3 wt%. Compared with the low-density Ni_1/NC, this increased in loading leads to an increase in active sites, resulting in a significant increase in CO current density. Yang et al. [82] used a high-temperature pyrolysis method to load Ni, Mn, Fe, Co, Cr, Cu, Zn, Ru and Pt atoms on carbon materials. Among them, they obtained Ni-SAC with a loading amount of 2.5 wt%, which exhibited high stability and excellent CO_2RR performance with respect to CO, with a Faraday efficiency of up to 99% at − 1.2 V. M-N_2C_2 SACs had excellent catalytic performance in CO_2RR due to their stable coordination environment and enhanced interaction between metal atoms and the carriers. Liu et al. [83]

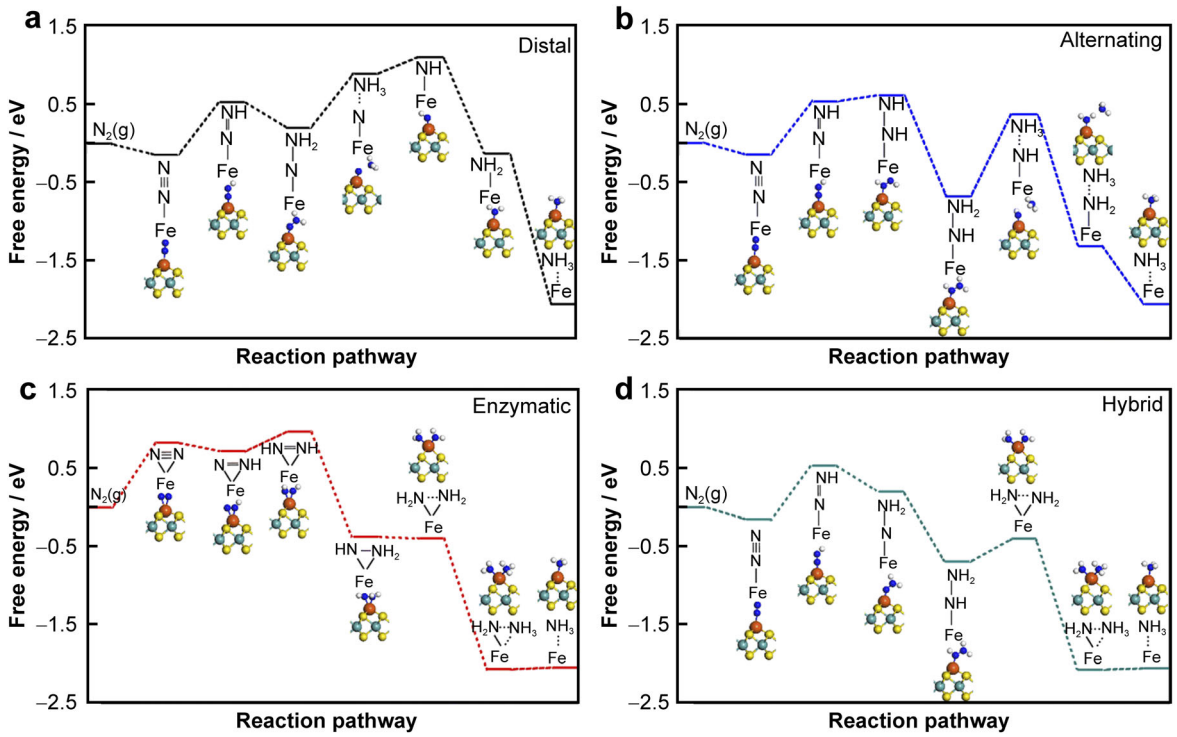

Fig. 10 Free energy diagram of NRR under different mechanisms with Fe_1/VS_2 as catalyst: **a** distal, **b** alternating, **c** enzymatic and **d** hybrid mechanisms. Reproduced with permission from Ref. [73]. Copyright 2022, Royal Society of Chemistry

reported a metal pre-buried strategy that could achieve both high loading and prevent the aggregation of metal atoms. The authors prepared Ni-NC-50 with a loading amount of 9.15 wt%. Through the analysis of X-ray fine structure spectroscopy experiments, it could be observed that the coordination structure of the catalyst was asymmetric (Fig. 11a). Moreover, the combination with XPS (Fig. 11b) allowed us to conclude that Ni sites existed in the form of atomic dispersion, a conclusion further supported by the WT k^3-weighted EXAFS spectra (Fig. 11c). In addition, Ni-NC-50 exhibited the highest charge transfer efficiency (Fig. 11e) and CO selectivity among the different loading amounts of Ni-NC. FE_{CO} was maintained at over 90% and could reach up to 98.7% (Fig. 11d).

CO_2RR is also an effective method to prepare high-value-added products using HLSAC. Cu-based catalysts have shown excellent performance in CO_2RR, particularly for the selectivity of C2 products. However, synthesizing single-atom Cu-based catalysts with good C–C coupling reaction is challenging as it requires multiple adjacent Cu sites [84]. However, Fontecave's team was able to successfully prepare a Cu–N–C catayst using a combination of ball milling and pyrolysis, with stable Cu–N_4 active sites that could effectively electrocatalyze CO_2 to ethanol, with a maximum FE of 43% [85]. This achievement opens up new possibilities for preparing diversified C2 products using single-atom Cu-based catalysts. Though it is still a challenge to synthesize high-value-added products other than CO using HLSAC, Cu-based catalysts have good selectivity for hydrocarbons and alcohols. With further structural adjustments, it is possible to achieve various C2 products in the future.

3.1.4 OER

Oxygen evolution reaction (OER) is the process of converting water molecules or hydroxide ions into oxygen gas by using electric energy. It is an important reaction step in water electrolysis systems, rechargeable metal–air batteries, etc. [86, 87]. The reaction occurs through four electron transfers, with different equations in acidic and alkaline environments. In acidic conditions, the reaction equation is: $2H_2O \rightarrow O_2 + 4H^+ + 4e^-$; while in alkaline conditions, it is: $4OH^- \rightarrow O_2 + 2H_2O + 4e^-$. OER can proceed through two possible mechanisms: adsorbate evolution mechanism (AEM) and lattice oxygen-mediated mechanism (LOM), involving the formation of oxygen intermediates such as O*, HO* and HOO*.

Efficient and stable catalysts are crucial in reducing the overpotential of OER and improving water electrolysis for hydrogen production [88, 89]. At present, HLSACs have made important progress in enhancing OER performance. For instance, Kumar and co-workers [36] reported a high-density Co SAC with a loading amount of 10.6 wt% for

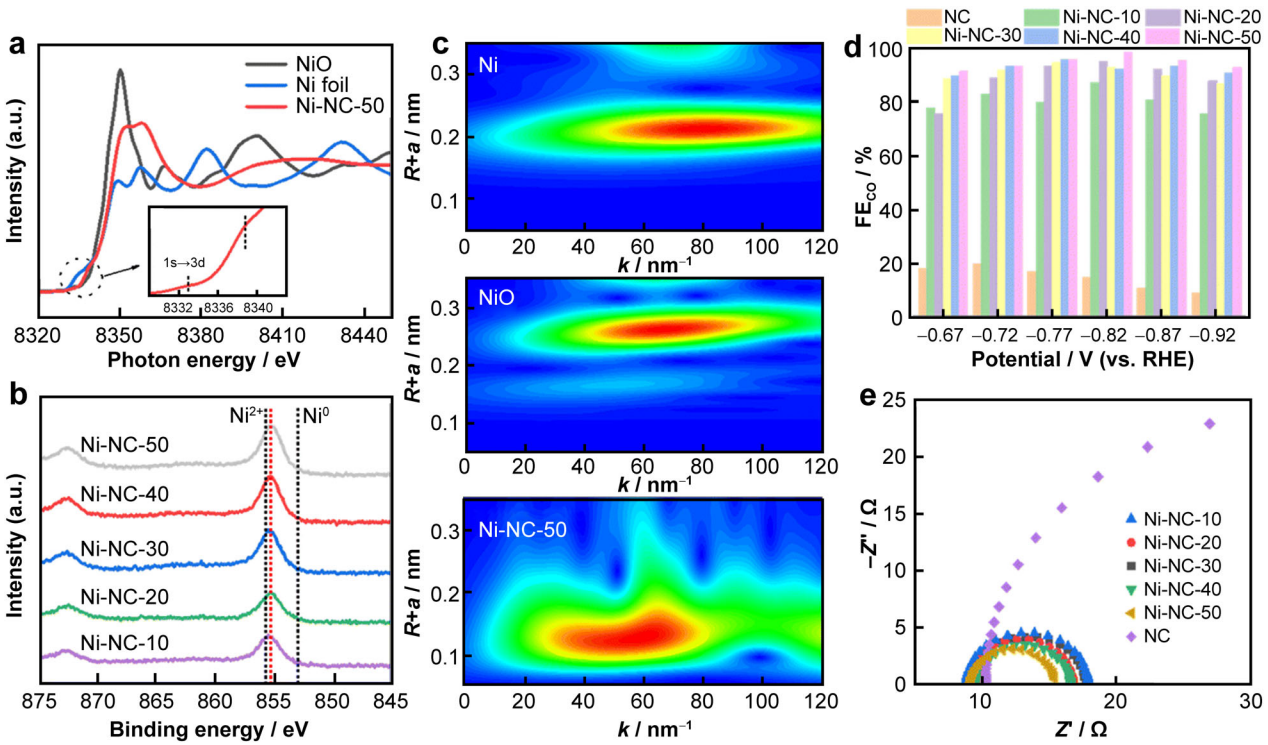

Fig. 11 CO_2RR performance of HLSACs: **a** Ni K-edge XANES spectra; **b** high-definition image of 2p electron level of Ni measured by XPS; **c** WT k^3-weighted EXAFS spectra; **d** FE_{CO} of NC, Ni-NC-10, Ni-NC-20, Ni-NC-30, Ni-NC-40 and Ni-NC-50 catalysts and **e** EIS measurement data. Reproduced with permission from Ref. [83]. Copyright 2022, Royal Society of Chemistry

OER. The catalyst consisted of atomically dispersed Co atoms supported on a high-porosity carbon network rich in N. As shown in Fig. 12a, the Co SAC exhibited a lower overpotential of 351 mV than commercial catalysts in 1 mol·L^{-1} KOH solution. It also demonstrated a high mass activity of 2209 mA·mg_{Co}^{-1} at 1.65 V/0.37 s^{-1} (Fig. 12b) and excellent stability (Fig. 12c). To understand the catalytic mechanism, the authors utilized operando X-ray absorption spectroscopy (XAS) analysis and observed the formation of an active intermediate, Co–O, which accelerated the OER kinetics (Fig. 12d and e). Additionally, DFT calculations revealed that the Co–N_4 coordination structure exhibited small energy changes and facilitated electron transport, contributing to its excellent OER performance (Fig. 12f). Overall, these findings highlighted the significant progress made by HLSACs in enhancing the efficiency of OER and the importance of selecting efficient, stable and selective catalysts to reduce overpotential.

3.2 Thermocatalysis

Thermal catalysis is an important area of research that focuses on using catalysts to facilitate chemical reactions under the influence of heat. The aim is to lower the activation energy, enhance reaction rates and improve selectivity. Developing catalysts with exceptional catalytic performance is crucial in achieving these goals. HLSACs have shown great potential in thermal catalysis applications, including catalytic oxidation and selective hydrogenation.

Catalytic oxidation reactions involve the introduction of oxygen atoms into organic or inorganic compounds using catalysts in the presence of oxygen or other oxidizing agents. This process leads to the production of valuable chemicals or environmentally friendly products [90–92]. Olefin epoxidation, for instance, plays a significant role in organic synthesis and pharmaceutical industries. It involves incorporating oxygen atoms into the double bonds of olefins to obtain important intermediates. Compared to traditional olefin epoxidation catalysts, HLSACs offer advantages such as higher efficiency, improved stability and environmental friendliness. For example, Xiong et al. [27] developed a catalyst consisting of 30 wt% Fe single-atom sites (SAS-Fe) for the epoxidation of styrene. This catalyst achieved a yield of 64% and a selectivity of 89% toward styrene oxide. The use of SAS-Fe led to higher selectivity for styrene oxidation than that of benzaldehyde. Another study conducted by Jin et al. [93] investigated the effect of different loading of Co SACs (range from 5.4 wt% to 21.2 wt%) on olefin epoxidation, specifically trans-stilbene epoxidation. The AC HAADF-STEM images of Co SAC with 21.2 wt% load are shown in Fig. 13a, where Co

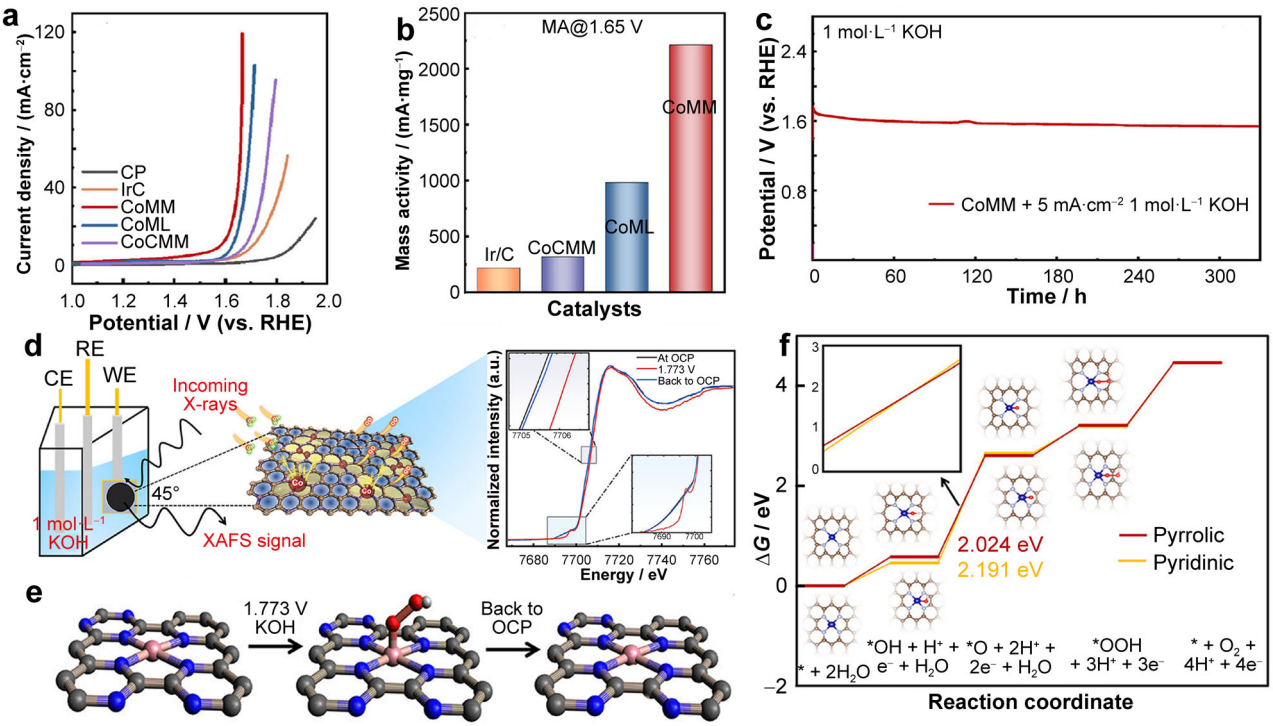

Fig. 12 OER performance of HLSACs: **a** LSV plot at 5 $mV \cdot s^{-1}$; **b** mass activity; **c** analyze schematic of CoMM using XAS method; **d** changes in chemical state of CoMM and **e, f** OER free energy spectroscopy and monatomic model of pyridine-nitrogen-cobalt. Reproduced with permission from Ref. [36]. Copyright 2023, American Chemical Society

atoms were densely distributed but isolated. And from Fig. 13b, it could be seen that higher Co loading resulted in improved catalytic activity. With Co SACs at 21.2 wt% loading, the conversion rate of reactants reached close to 100% within 1 h. The catalytic mechanism was also studied, and DFT calculations revealed a positive correlation between the activation of O_2 molecules and trans-stilbene with the charge density of Co single atoms (Fig. 13c and d). These examples demonstrate the potential of HLSACs in catalytic oxidation reactions and highlight their superior performance compared to conventional catalysts. Such advancements provide valuable insights into optimizing catalytic processes and furthering the development of thermal catalysis.

Selective hydrogenation is a process that involves reducing organic compounds containing reducible functional groups to produce target products with significant applications in several fields, such as petrochemicals. The selection of catalysts for this reaction is crucial, and SACs have garnered significant attention due to their high activity and selectivity [94]. For example, Yan et al. [54] prepared Co_1/G SACs with high activity and selectivity for nitroaromatic hydrogenation using graphene as a support material. The metal loading of this catalyst was 5 wt%. The active center of the catalyst was positively charged Co–O–C, which had weak adsorption to diazo compounds, resulting in incomplete hydrogenation of the products. Li et al. [95] synthesized Pd SACs with a load of 5.6 wt% and a bamboo-like structure, which demonstrated good conversion rate and selectivity in the semi-hydrogenation of phenylacetylene. This catalyst possessed a three-layer porous structure, with the main channel comprised of hollow nanofibers, and numerous parallel and vertical secondary channels presented between the nanofibers and on the fiber walls, as well as micropores distributed on the channel surface. This complex structure provided the catalyst with a high specific surface area and porosity, facilitating the loading of single atoms and full exposure of active sites, thereby improving its catalytic performance.

3.3 Photocatalysis

Photocatalysis is a process that uses light energy to induce chemical reactions, including the decomposition of organic pollutants, CO_2, water to produce harmless or valuable chemicals. The photocatalyst is a crucial component that converts light energy into charge carriers, promoting redox reactions. SACs have demonstrated remarkable performance in various photocatalytic reactions, including water splitting [96–98], nitrogen fixation [99, 100], owing to their ability to enhance the charge utilization efficiency, activity and selectivity of processes [101, 102].

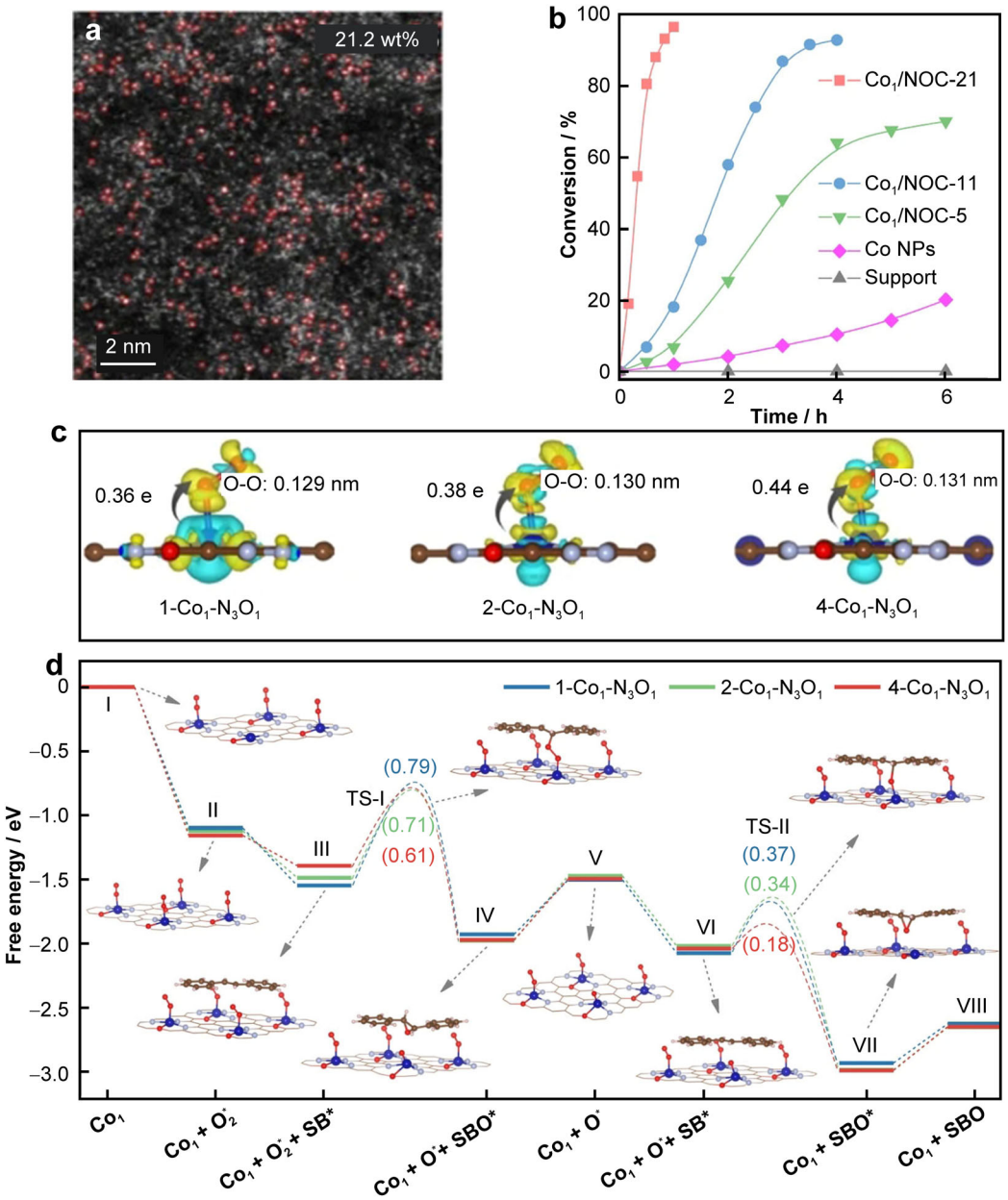

Fig. 13 Thermocatalysis performance of HLSACs: **a** AC HAADF-STEM images of 21.2 wt% Co SAC; **b** plotting of trans-stilbene in different samples with reaction time; **c** illustration of charge density difference between O_2 adsorption in different *x*-Co_1-N_3O_1 models and **d** reaction energy barrier of trans-stilbene epoxidation reactions of *x*-Co_1-N_3O_1. Reproduced with permission from Ref. [93]. Copyright 2023, Nature Publishing Group

HLSACs bound with MOFs and carbon-based materials as carriers have been developed for use in photocatalysis. MOFs are excellent support materials that cooperate with densely distributed metal single atoms to demonstrate outstanding performance in photocatalytic hydrogen production [103, 104]. Fang et al. [105] successfully used an aluminum-based porphyrin MOF as a support material probably for the first time, confining Pt single atoms to create Al-TCPP-Pt SACs with hydrogen production activity superior to that of Al-TCPP-Pt NPs, despite having only 0.07 wt% of Pt loading. Similarly, Zuo et al. [60] utilized 2D ultra-thin MOF nanosheets as carriers to synthesize PtSA-MNSs with a loading amount of 12.0 wt% through a coordination stabilization strategy. As depicted in Fig. 14a, the resulting photocatalyst exhibited a record-breaking hydrogen production rate of 11,320 $\mu mol \cdot g^{-1} \cdot h^{-1}$. According to DFT calculations, PtSA-MNSs can generate effective electron transfer channels, facilitating

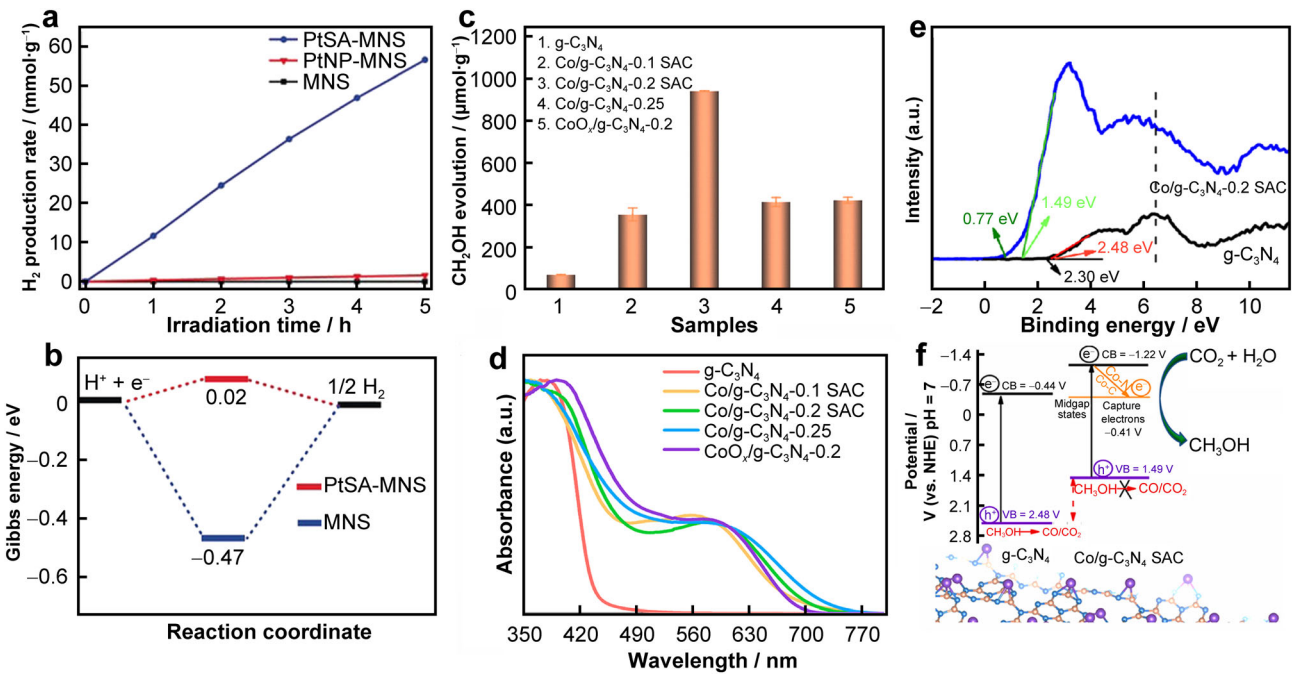

Fig. 14 Photocatalysis performance of HLSACs. **a** Photocatalytic hydrogen production rates of Pt SA-MNSs, Pt NP-MNS and MNSs catalysts under photocatalytic-like conditions and **b** DGH* on MNSs and Pt SA-MNSs. Reproduced with permission from Ref. [60]. Copyright 2019, Wiley–VCH GmbH. **c** Photocatalytic yield of carbon dioxide to ethanol; **d** UV–Vis diffuse reflectance spectrogram; **e** XPS valence band and **f** band structure. Reproduced with permission from Ref. [106]. Copyright 2021 Elsevier B.V

hydrogen production (Fig. 14b). This approach represented the first instance of a 2D MOF being used for a single-atom photocatalyst.

Carbon-based materials, known for their high specific surface area and conductivity, have wide-ranging applications. When employed as photocatalytic carriers, carbon-based materials can enhance light absorption range and reaction activity. For example, Ma et al. [106] adopted a pyrolysis–induction–evaporation strategy to fabricate ultra-high-density Co/g-C_3N_4 SACs, demonstrating high activity and selectivity in the photocatalytic conversion of CO_2 to methanol. The resulting catalyst, Co/g-C_3N_4-0.2 SACs, exhibited a Co loading of 29.3 wt% and achieved a methanol production rate of 941.9 μmol·g^{-1} under light irradiation, maintaining good photocatalytic activity for up to 48 h (Fig. 14c). Co/g-C_3N_4 SACs facilitated methanol production through the presence of ultra-high-density Co-N_2C active sites, which significantly extended the light absorption range (Fig. 14d). XPS valence band (Fig. 14e) and band structure (Fig. 14f) analyses conducted by the authors verified that the Co-N_2C sites not only accumulated numerous electrons but also adsorbed and activated CO_2. In addition, Shi and co-workers [107] synthesized Co SAC using porous nitrogen-doped carbon materials as support, with a Co loading amount of 5.9 wt%, and used them as photocatalytic catalysts for hydrogen production. The catalysts displayed a hydrogen production rate of 1180 μ·mol·g^{-1}·h^{-1}.

HLSACs play a vital role in advancing energy electrocatalysis, contributing significantly to the development of efficient and sustainable energy conversion technologies. Table 1 presents a summary of HLSACs synthesized using different methods in the field of electrocatalysis [22, 26, 32, 36, 42, 48, 50, 56, 69, 70, 74, 75, 86, 95, 96, 108–118].

4 Conclusions and outlook

HLSACs are a novel type of catalytic materials that exhibit excellent catalytic activity and selectivity in various catalytic applications. The reasons for their superior performance are mainly attributed to the following three aspects: Firstly, SACs themselves have high atomic utilization efficiency, which can fully exploit the catalytic potential of metals and greatly improve the catalytic efficiency; secondly, the increase in loading amount leads to the exposure of more active sites on the catalyst surface, which facilitates the enhancement of catalytic rate and selectivity; thirdly, HLSACs are prepared using suitable synthesis strategies, resulting in a significant improvement of catalyst stability, due to that the carriers or specific templates with abundant anchoring sites can anchor the metal atoms, strengthen the metal-carrier interaction and prevent the aggregation of metals.

Table 1 Recent advances of HLSACs with different synthesis methods

Application	Metal	SACs	Loading (wt%, ICP)	Synthetic method	Refs.
ORR	Pt	h-Pt_1-CuS_x	24.8 at%	Ion exchange method	[50]
		Pt/ZTC	5.0	Wet impregnation method	[108]
	Fe	Fe-NC SAC	8.9	Cascade anchoring strategy	[26]
		ISA Fe/CN	2.16	Cage-encapsulated-precursor pyrolysis strategy	[32]
		Fe SA/NCZ	4.3	Pyrolysis	[109]
		Fe SAs-PNCF	5.48	Pyrolysis	[110]
		SAC-Fe/NC	8.5	Plasma bombing strategy	[111]
	Cu	Cu–N–C	20.9	Pyrolysis	[86]
	Co	Co SAs-PNCF	4.32	Pyrolysis	[96]
		Co_{40}SAs/AC@NG	14.0	Pyrolysis	[56]
		Co–N–B–C	4.2	Pyrolysis	[115]
		Co-SAC/G	4.12	Single-atom coating strategy	[116]
NRR	Cu	NC-Cu SA	5.31	Facile surfactant-assisted	[70]
	Rh	Rh SA/GDY	13.22	One-pot synthetic method	[69]
	Ru	Ru SA/GDY	15.31	One-pot synthetic method	[69]
	Co	Co SA/GDY	12.08	One-pot synthetic method	[69]
	Mo	SA-Mo/NPC	9.54	In situ synthesis approach	[22]
CO_2RR	Ni	Ni SAs/N–C	1.53	Ion exchange-pyrolysis method	[112]
		Ni-SAC	2.5	Ligand-mediated method	[74]
		Ni–NC-50	9.15	Metal pre-buried strategy	[75]
	Cu	Cu_1/PCN	21.8	Wet-chemistry method	[48]
		UHD-SAC			
OER	Fe	Fe SA/NCZ	4.3	Pyrolysis	[95]
	Ir	Ir-NiO	~ 18	Wet-chemistry method	[113]
		Ir_1/$Co(OH)_2$	2.6 at%	One-step strategy	[117]
	Co	Co-N_4 SAC	10.6	Macromolecule-assisted	[36]
HER	Pt	Pt SAC-N_xC_y	5.31	Cascade anchoring strategy	[114]
		Pt SAs/DG	2.1	CVD-assisted	[42]
		Pt_1/$Co(OH)_2$	1.9 at%	One-step strategy	[117]
	Ru	PCN-$Rh_{15.9}$/KB	15.9	Pyrolysis	[118]

In this review, we initially summarized and discussed common synthesis strategies for SACs with a loading of more than 1 wt%, which are generally divided into top-down and bottom-up strategies. In the top-down approach, we further classify it into thermalchemical methods (confinement pyrolysis strategy, CVD) and electrochemical methods (electrodeposition method). In the bottom-up approach, we classify it into wet chemical methods (co-precipitation, impregnation and ion exchange), ALD and pyrolysis, etc. Among the various synthesis methods introduced, we can see that the pyrolysis method is an effective and feasible approach for preparing HLSACs, while the HLSACs prepared by the deposition method have lower loading. Then, we reviewed and summarized the applications of HLSACs and elaborated on some important catalytic mechanisms. HLSACs have superior performance in electrocatalysis (OER, ORR, NRR and CO_2RR), thermocatalysis and photocatalysis compared to low-loading SACs and conventional catalysts. At present, significant achievements have been made in the research of HLSACs, such as new synthesis methods that can synthesize higher-loading SACs, or better catalytic performance, further improvements are still possible.

The preparation of high metal loading SACs mainly involves two aspects: One is to disperse the abundant metal single atoms and avoid aggregation, and the other is to anchor the dispersed metal atoms on carriers with rich defect sites. Commonly used carriers include MOF materials, graphene, nitrogen-doped carbon materials, etc. While some studies have successfully used a simple dangling bond capture strategy to prepare SACs with high loading suitable for industrial applications, this method is not universally applicable. Therefore, in order to achieve widespread preparation of HLSACs, researchers need to

propose more optimized synthesis strategies. Furthermore, researchers also need to explore additional carriers that can effectively immobilize densely dispersed single atoms. Various supports are being studied, including oxides (such as CeO_2), ion exchange resins, MOFs and carbon-based materials, among which carbon-based materials are the most widely used. The paper mentioned Pt SACs with the highest loading prepared by the laser implantation method on GQDs.

The performance of HLSACs varies depending on the specific combination of metals and carriers, and they exhibit different advantages in different catalytic applications. Moreover, the selectivity of catalytic products is also influenced by various reaction conditions. To address these challenges, it is crucial to explore the mechanisms of HLSACs in different catalytic reactions. This research has significant implications for enhancing the performance and expanding the application scope of HLSACs. Currently, it is known that the local environment surrounding the catalyst plays a crucial role in determining its active center and catalytic performance. There exists a complex interaction between the catalytic active center and the carrier material. However, this also gives rise to several questions. For instance, how do different coordination environments impact the electronic structure and reactivity of the catalytic active center? How are these interactions formed and regulated? Researchers need to conduct further investigations to address these issues.

The characterization of general materials mainly includes micro-morphology characterization, phase analysis, composition characterization, thermal property analysis and mechanical property testing. For nanomaterials, we mainly focus on the first three aspects. Among them, the methods for observing the surface or compound content and distribution of nanomaterials include: SEM, TEM, AFM, etc.; the methods for determining the phase composition and crystal structure of nanomaterials include: XRD, Raman spectroscopy, nuclear magnetic resonance (NMR) and selected area electron diffraction (SAED), etc; and the methods for measuring the element content and distribution in materials include: XPS, ICP-MS, etc. When the material size reaches the atomic level, the resolution requirement of the instrument is higher, and the conventional means cannot meet it. At present, the characterization of single atoms is through AC HAADF STEM to observe the dispersion of atoms, through XAS to analyze the valence state, coordination number and coordination environment of single atoms; through infrared spectroscopy (IR) to study the interaction of single atoms with carriers and reactants; through in situ TEM to monitor the structure and dynamics of single atoms under reaction conditions, etc. Although these means provide convenience for the characterization of SACs to some extent, they also have some limitations. For example, limited by the synchrotron radiation source, XAS is difficult to be widely used, and the mechanism explanation part needs more theoretical support; in situ characterization methods have many influencing factors and have strict requirements on instrument equipment. More importantly, the characterization technology of SACs is generally costly and difficult to popularize. Therefore, the research on the characterization means of SACs is a long-term process. It is necessary to improve the existing characterization technology, reduce the research cost and explore new characterization methods.

Acknowledgements This study was financially supported by Beijing Natural Science Foundation (No. 2212018), Beijing Institute of Technology Research Fund Program for Young Scholars (No. 2022CX01011), Ningbo 3315 Innovative Teams Program (No. 2019A-14-C), the National Natural Science Foundation of China (No. 12374390), the Member of Youth Innovation Promotion Association Foundation of CAS, China (No. 2023310) and the Key Scientific and Technological Special Project of Ningbo City No. (2023Z209).

Declarations

Conflict of interests The authors declare that they have no conflict of interest.

References

[1] Wang JH, Yang SW, Ma FB, Zhao YK, Zhao SN, Xiong ZY, Cai D, Shen HD, Zhu K, Zhang QY, Cao YL, Wang TS, Zhang HP. RuCo alloy nanoparticles embedded within N-doped porous two-dimensional carbon nanosheets: a high-performance hydrogen evolution reaction catalyst. Tungsten. 2023. https://doi.org/10.1007/s42864-023-00223-3.

[2] Liu J, Wang SL, Xuan JL, Shan BF, Luo H, Deng LP, Yang P, Qi CZ. Preparation of tungsten–iron composite oxides and application in environmental catalysis for volatile organic compounds degradation. Tungsten. 2022;4(1):38. https://doi.org/10.1007/s42864-021-00128-z.

[3] Li R, Ling L, Zhang W. Single iron atom catalysis: an environmental perspective. Nano Today. 2021;38:101117. https://doi.org/10.1016/j.nantod.2021.101117.

[4] Chen JJ, Gu S, Hao R, Wang ZY, Li MQ, Li ZQ, Liu K, Liao KM, Wang ZQ, Huang H, Li YZ, Zhang KL, Lu ZG. Co single atoms and nanoparticles dispersed on N-doped carbon nanotube as high-performance catalysts for Zn-air batteries. Rare Met. 2022; 41:2055. https://doi.org/10.1007/s12598-022-01974-7.

[5] Liu H, Li D, Guo J, Li Y, Liu A, Bai Y, He D. Recent advances on catalysts for preferential oxidation of CO. Nano Res. 2023; 16(4):4399. https://doi.org/10.1007/s12274-022-5182-9.

[6] Han J, Guan J. Heteronuclear dual-metal atom catalysts for nanocatalytic tumor therapy. Chinese J Catal. 2023;47:1. https://doi.org/10.1016/S1872-2067(22)64207-4.

[7] Guo W, Tong T, Liu X, Guo Y, Wang Y. Morphology-tuned activity of Ru/Nb_2O_5 catalysts for ketone reductive amination. ChemCatChem. 2019;11(16):4130. https://doi.org/10.1002/cctc.201900335.

[8] Wang S, Yan W, Zhao F. Recovery of solid waste as functional heterogeneous catalysts for organic pollutant removal and biodiesel production. Chem Eng J. 2020;401(1):126104. https://doi.org/10.1016/j.cej.2020.126104.

[9] Chen CQ, Fan XS, Zhou C, Lin L, Luo Y, Au C, Cai GH, Wang XY, Jiang LL. Hydrogen production from ammonia decomposition over Ni/CeO_2 catalyst: effect of CeO_2 morphology. J Rare Earths. 2023;41(7):1014. https://doi.org/10.1016/j.jre.2022.05.001.
[10] Zhao W, Shen J, Xu X, He W, Liu L, Chen Z, Liu J. Functional catalysts for polysulfide conversion in Li-S batteries: from micro/nanoscale to single atom. Rare Met. 2022;41(4):1080. https://doi.org/10.1007/s12598-021-01865-3.
[11] Liu JB, Gong HS, Ye GL, Fei HL. Graphene oxide-derived single-atom catalysts for electrochemical energy conversion. Rare Met. 2022;41(5):1703. https://doi.org/10.1007/s12598-021-01904-z.
[12] Cui X, Li W, Ryabchuk P, Junge K, Beller M. Bridging homogeneous and heterogeneous catalysis by heterogeneous single-metal-site catalysts. Nat Catal. 2018;1(6):385. https://doi.org/10.1038/s41929-018-0090-9.
[13] Chen F, Jiang X, Zhang L, Lang R, Qiao B. Single-atom catalysis: bridging the homo- and heterogeneous catalysis. Chinese J Catal. 2018;39(5):893. https://doi.org/10.1016/s1872-2067(18)63047-5.
[14] Mitchell S, Thomasb JM, Pérez-Ramírez J. Single atom catalysis. Catal. Sci Technol. 2017;7(19):4248. https://doi.org/10.1039/C7CY90090B.
[15] Chen G, Sciortino F, Ariga K. Atomic nanoarchitectonics for catalysis. Adv Mater Interfaces. 2021;8(8):2001395. https://doi.org/10.1002/admi.202001395.
[16] Yang X, Wang A, Qiao B, Li J, Liu J, Zhang T. Single-atom catalysts: a new frontier in heterogeneous catalysis. Acc Chem Res. 2013;46(8):1740. https://doi.org/10.1021/ar300361m.
[17] Maschmeyer T, Rey F, Sankar G, Thomas JM. Heterogeneous catalysts obtained by grafting metallocene complexes onto mesoporous silica. Nature. 1995;378(6553):159. https://doi.org/10.1038/378159a0.
[18] Qiao B, Wang A, Yang X, Allard LF, Jiang Z, Cui Y, Liu J, Li J, Zhang T. Single-atom catalysis of CO oxidation using Pt_1/FeO_x. Nat Chem. 2011;3(8):634. https://doi.org/10.1038/nchem.1095.
[19] Yin P, Yao T, Wu Y, Zheng L, Lin Y, Liu W, Ju H, Zhu J, Hong X, Deng Z, Zhou G, Wei S, Li Y. Single cobalt atoms with precise n-coordination as superior oxygen reduction reaction catalysts. Angew Chem Int Ed. 2016;55(36):10800. https://doi.org/10.1002/anie.201604802.
[20] Cheon JY, Kim JH, Kim JH, Goddeti KC, Park JY, Joo SH. Intrinsic relationship between enhanced oxygen reduction reaction activity and nanoscale work function of doped carbons. J Am Chem Soc. 2014;136(25):8875. https://doi.org/10.1021/ja503557x.
[21] Sahraie NR, Kramm UI, Steinberg J, Zhang Y, Thomas A, Reier T, Paraknowitsch J, Strasser P. Quantifying the density and utilization of active sites in non-precious metal oxygen electroreduction catalysts. Nat Commun. 2015;6(1):8618. https://doi.org/10.1038/ncomms9618.
[22] Han L, Liu X, Chen J, Lin R, Liu H, Lü F, Bak S, Liang Z, Zhao S, Stavitski E, Luo J, Adzic RR, Xin HL. Atomically dispersed molybdenum catalysts for efficient ambient nitrogen fixation. Angew Chem Int Ed. 2019;58(8):2321. https://doi.org/10.1002/anie.201900203.
[23] Geng Z, Liu Y, Kong X, Li P, Li K, Liu Z, Du J, Shu M, Si R, Zeng J. Achieving a record-high yield rate of 120.9 $\mu g_{NH3} \cdot mg_{cat.}^{-1} \cdot h^{-1}$ for N_2 electrochemical reduction over Ru single-atom catalysts. Adv Mater. 2018;30(40):1803498. https://doi.org/10.1002/adma.201803498.
[24] Qiu W, Xie X, Qiu J, Fang W, Liang R, Ren X, Ji X, Cui G, Asiri AM, Cui G, Tang B, Sun X. High-performance artificial nitrogen fixation at ambient conditions using a metal-free electrocatalyst. Nat Commun. 2018;9(1):3485. https://doi.org/10.1038/s41467-018-05758-5.
[25] Chen S, Perathoner S, Ampelli C, Mebrahtu C, Su D, Centi G. Room-temperature electrocatalytic synthesis of NH_3 from H_2O and N_2 in a gas–liquid–solid three-phase reactor. ACS Sustain Chem Eng. 2017;5(8):7393. https://doi.org/10.1021/acssuschemeng.7b01742.
[26] Zhao L, Zhang Y, Huang L, Liu X, Zhang Q, He C, Wu Z, Zhang L, Wu J, Yang W, Gu L, Hu J, Wan L. Cascade anchoring strategy for general mass production of high-loading single-atomic metal-nitrogen catalysts. Nat Commun. 2019;10(1):1278. https://doi.org/10.1038/s41467-019-09290-y.
[27] Xiong Y, Sun W, Xin P, Chen W, Zheng X, Yan W, Zheng L, Dong J, Zhang J, Wang D, Li Y. Gram-scale synthesis of high-loading single-atomic-site Fe catalysts for effective epoxidation of styrene. Adv Mater. 2020;32(34):2000896. https://doi.org/10.1002/adma.202000896.
[28] Jia B, Bai L, Han Z, Li R, Huangfu J, Li C, Zheng J, Qu Y, Leng K, Wang Y, Bai J. High-performance styrene epoxidation with vacancy-defect cobalt single-atom catalysts. ACS Appl Mater Inter. 2022;14(8):10337. https://doi.org/10.1021/acsami.1c23079.
[29] Xia C, Qiu Y, Xia Y, Zhu P, King G, Zhang X, Wu Z, Kim JY, Cullen DA, Zheng D, Li P, Shakouri M, Heredia E, Cui P, Alshareef HN, Hu Y, Wang H. General synthesis of single-atom catalysts with high metal loading using graphene quantum dots. Nat Chem. 2021;13(9):887. https://doi.org/10.1038/s41557-021-00734-x.
[30] Li Z, Li B, Hu Y, Liao X, Yu H, Yu C. Emerging ultrahigh-density single-atom catalysts for versatile heterogeneous catalysis applications: redefinition, recent progress, and challenges. Small Struct. 2022;3(6):2200041. https://doi.org/10.1002/sstr.202200041.
[31] Sangkhun W, Ponchai J, Phawa C, Pengsawang A, Faungnawakij K, Butburee T. Race on high-loading metal single atoms and successful preparation strategies. ChemCatChem. 2022;14(2):e202101266.https://doi.org/10.1002/cctc.202101266.
[32] Chen Y, Ji S, Wang Y, Dong J, Chen W, Li Z, Shen R, Zheng L, Zhuang Z, Wang D, Li Y. Isolated single iron atoms anchored on n-doped porous carbon as an efficient electrocatalyst for the oxygen reduction reaction. Angew Chem Int Ed. 2017;56(24):6937. https://doi.org/10.1002/anie.201702473.
[33] Liu J, Xiao H, Li J. Constructing high-loading single-atom/cluster catalysts via an electrochemical potential window strategy. J Am Chem Soc. 2020;142(7):3375. https://doi.org/10.1021/jacs.9b06808.
[34] Jin Z, Li P, Meng Y, Fang Z, Xiao D, Yu G. Understanding the inter-site distance effect in single-atom catalysts for oxygen electroreduction. Nat Catal. 2021;4(7):615. https://doi.org/10.1038/s41929-021-00650-w.
[35] Mehmood A, Gong M, Jaouen F, Roy A, Zitolo A, Khan A, Sougrati M, Primbs M, Bonastre AM, Fongalland D, Drazic G, Strasser P, Kucernak A. High loading of single atomic iron sites in Fe-NC oxygen reduction catalysts for proton exchange membrane fuel cells. Nat Catal. 2022;5(4):311. https://doi.org/10.1038/s41929-022-00772-9.
[36] Kumar P, Kannimuthu K, Zeraati AS, Roy S, Wang X, Wang X, Samanta S, Miller KA, Molina M, Trivedi D, Abed J, Campos Mata MA, Al-Mahayni H, Baltrusaitis J, Shimizu G, Wu YA, Seifitokaldani A, Sargent EH, Ajayan PM, Hu J, Kibria MG. High-density cobalt single-atom catalysts for enhanced oxygen evolution reaction. J Am Chem Soc. 2023;145(14):8052. https://doi.org/10.1021/jacs.3c00537.
[37] Wang K, Wang X, Liang X. Synthesis of high metal loading single atom catalysts and exploration of the active center

structure. ChemCatChem. 2021;13(1):28. https://doi.org/10.1002/cctc.202001255.
[38] Jones J, Xiong H, Delariva AT, Peterson EJ, Pham H, Challa SR, Qi G, Oh S, Wiebenga MH, Pereira Hernández XI, Wang Y, Datye AK. Thermally stable single-atom platinum-on-ceria catalysts via atom trapping. Science. 2016;353(6295):150. https://doi.org/10.1126/science.aaf8800.
[39] Liu J, Cao C, Liu X, Zheng L, Yu X, Zhang Q, Gu L, Qi R, Song W. Direct observation of metal oxide nanoparticles being transformed into metal single atoms with oxygen-coordinated structure and high-loadings. Angew Chem Int Ed. 2021;60(28):15248. https://doi.org/10.1002/anie.202102647.
[40] Maury F, Alexandrov S, Barreca D, Davazoglou D, Pemble M. In recognition of professor hitchman: advances in chemical vapor deposition. Adv Mater Interfaces. 2017;4(18):1700984. https://doi.org/10.1002/admi.201700984.
[41] Arnault J, Saada S, Ralchenko V. Chemical vapor deposition single-crystal diamond: a review. Phy status solidi RRL. 2022;16(1):2100354. https://doi.org/10.1002/pssr.202100354.
[42] Qu Y, Chen B, Li Z, Duan X, Wang L, Lin Y, Yuan T, Zhou F, Hu Y, Yang Z, Zhao C, Wang J, Zhao C, Hu Y, Wu G, Zhang Q, Xu Q, Liu B, Gao P, You R, Huang W, Zheng L, Gu L, Wu Y, Li Y. Thermal emitting strategy to synthesize atomically dispersed Pt metal sites from bulk Pt metal. J Am Chem Soc. 2019;141(11):4505. https://doi.org/10.1021/jacs.8b09834.
[43] Qu Y, Li Z, Chen W, Lin Y, Yuan T, Yang Z, Zhao C, Wang J, Zhao C, Wang X, Zhou F, Zhuang Z, Wu Y, Li Y. Direct transformation of bulk copper into copper single sites via emitting and trapping of atoms. Nat Catal. 2018;1(10):781. https://doi.org/10.1038/s41929-018-0146-x.
[44] Gao D, Li H, Wei P, Wang Y, Wang G, Bao X. Electrochemical synthesis of catalytic materials for energy catalysis. Chinese J Catal. 2022;43(4):1001. https://doi.org/10.1016/S1872-2067(21)63940-2.
[45] Zhang L, Han L, Liu H, Liu X, Luo J. Potential-cycling synthesis of single platinum atoms for efficient hydrogen evolution in neutral media. Angew Chem Int Ed. 2017;56(44):13694. https://doi.org/10.1002/ange.201706921.
[46] Qu Y, Wang L, Li Z, Li P, Zhang Q, Lin Y, Zhou F, Wang H, Yang Z, Hu Y, Zhu M, Zhao X, Han X, Wang C, Xu Q, Gu L, Luo J, Zheng L, Wu Y. Ambient synthesis of single-atom catalysts from bulk metal via trapping of atoms by surface dangling bonds. Adv Mater. 2019;31(44):1904496. https://doi.org/10.1002/adma.201904496.
[47] Zarkov A, Kareiva A, Tamasauskaite-Tamasiunaite L. Advances in functional inorganic materials prepared by wet chemical methods. Crystals. 2021;11(8):943. https://doi.org/10.3390/cryst11080943.
[48] Hai X, Xi S, Mitchell S, Harrath K, Xu H, Akl DF, Kong D, Li J, Li Z, Sun T, Yang H, Cui Y, Su C, Zhao X, Li J, Pérez-Ramírez J, Lu J. Scalable two-step annealing method for preparing ultra-high-density single-atom catalyst libraries. Nat Nanotechnol. 2022;17(2):174. https://doi.org/10.1038/s41565-021-01022-y.
[49] Kunwar D, Zhou S, Delariva A, Peterson EJ, Xiong H, Pereira-Hernández XI, Purdy SC, ter Veen R, Brongersma HH, Miller JT, Hashiguchi H, Kovarik L, Lin S, Guo H, Wang Y, Datye AK. Stabilizing high metal loadings of thermally stable platinum single atoms on an industrial catalyst support. ACS Catal. 2019;9(5):3978. https://doi.org/10.1021/acscatal.8b04885.
[50] Shen R, Chen W, Peng Q, Lu S, Zheng L, Cao X, Wang Y, Zhu W, Zhang J, Zhuang Z, Chen C, Wang D, Li Y. High-concentration single atomic Pt sites on hollow CuS_x for selective O_2 reduction to H_2O_2 in acid solution. Chem-Us. 2019;5(8):2099. https://doi.org/10.1016/j.chempr.2019.04.024.
[51] Graniel O, Weber M, Balme S, Miele P, Bechelany M. Atomic layer deposition for biosensing applications. Biosens Bioelectron. 2018;122:147. https://doi.org/10.1016/j.bios.2018.09.038.
[52] Hu L, Qi W, Li Y. Coating strategies for atomic layer deposition. Nanotechnol Rev. 2017;6(6):527. https://doi.org/10.1515/ntrev-2017-0149.
[53] Sun S, Zhang G, Gauquelin N, Chen N, Zhou J, Yang S, Chen W, Meng X, Geng D, Banis MN, Li R, Ye S, Knights S, Botton GA, Sham T, Sun X. Single-atom catalysis using Pt/graphene achieved through atomic layer deposition. Sci Rep-Uk. 2013;3(1):1775. https://doi.org/10.1038/srep01775.
[54] Yan H, Zhao X, Guo N, Lyu Z, Du Y, Xi S, Guo R, Chen C, Chen Z, Liu W, Yao C, Li J, Pennycook SJ, Chen W, Su C, Zhang C, Lu J. Atomic engineering of high-density isolated Co atoms on graphene with proximal-atom controlled reaction selectivity. Nat Commun. 2018;9(1):3197. https://doi.org/10.1038/s41467-018-05754-9.
[55] Wei G, Liu X, Zhao Z, Men C, Ding Y, Gao S. Constructing ultrahigh-loading unsymmetrically coordinated $Zn\text{-}N_3O$ single-atom sites with efficient oxygen reduction for H_2O_2 production. Chem Eng J. 2023;455(2):140721. https://doi.org/10.1016/j.cej.2022.140721.
[56] Zhang M, Li H, Chen J, Ma FX, Zhen L, Wen Z, Xu CY. High-loading Co single atoms and clusters active sites toward enhanced electrocatalysis of oxygen reduction reaction for high-performance Zn-air battery. Adv Funct Mater. 2023;33(4):2209726. https://doi.org/10.1002/adfm.202209726.
[57] Wang B, Zhu X, Pei X, Liu W, Leng Y, Yu X, Wang C, Hu L, Su Q, Wu C, Yao Y, Lin Z, Zou Z. Room-temperature laser planting of high-loading single-atom catalysts for high-efficiency electrocatalytic hydrogen evolution. J Am Chem Soc. 2023;145(25):13788. https://doi.org/10.1021/jacs.3c02364.
[58] Yang Q, Xu Q, Jiang HL. Metal-organic frameworks meet metal nanoparticles: synergistic effect for enhanced catalysis. Chem Soc Rev. 2017;46(15):4774. https://doi.org/10.1039/C6CS00724D.
[59] Hu M-L, Masoomi MY, Morsali A. Template strategies with MOFs. Coordin Chem Rev. 2019;387:415. https://doi.org/10.1016/j.ccr.2019.02.021.
[60] Zuo Q, Liu T, Chen C, Ji Y, Gong X, Mai Y, Zhou Y. Ultrathin metal-organic framework nanosheets with ultrahigh loading of single Pt atoms for efficient visible-light-driven photocatalytic H_2 evolution. Angew Chem Int Ed. 2019;58(30):10198. https://doi.org/10.1002/anie.201904058.
[61] Gong HY, Liang X, Sun GL, Li DW, Zheng XJ, Shi H, Zeng K, Xu GC, Li Y, Yang RZ, Yuan CZ. Insight into role of Ni/Fe existing forms in reversible oxygen catalysis based on Ni-Fe single-atom/nanoparticles and N-doped carbon. Rare Met. 2022;41(12):4034. https://doi.org/10.1007/s12598-022-02078-y.
[62] Jiao Y, Zheng Y, Jaroniec M, Qiao SZ. Origin of the electrocatalytic oxygen reduction activity of graphene-based catalysts: a roadmap to achieve the best performance. J Am Chem Soc. 2014;136(11):4394. https://doi.org/10.1021/ja500432h.
[63] Humayun M, Israr M, Khan A, Bououdina M. State-of-the-art single-atom catalysts in electrocatalysis: from fundamentals to applications. Nano Energy. 2023;113:108570. https://doi.org/10.1016/j.nanoen.2023.108570.
[64] Pang R, Xia H, Li J, Guo S, Wang E. Recent developments of atomically dispersed metal electrocatalysts for oxygen reduction reaction. Chinese J Chem. 2023;41(5):581. https://doi.org/10.1002/cjoc.202200488.
[65] Yan L, Li P, Zhu Q, Kumar A, Sun K, Tian S, Sun X. Atomically precise electrocatalysts for oxygen reduction reaction. Chem-Us. 2023;9(2):280. https://doi.org/10.1016/j.chempr.2023.01.003.

[66] Tong M, Wang L, Fu H. Designed synthesis and catalytic mechanisms of non-precious metal single-atom catalysts for oxygen reduction reaction. Small Methods. 2021;5(10): 2100865. https://doi.org/10.1002/smtd.202100865.
[67] Zhou Y, Tao X, Chen G, Lu R, Wang D, Chen M, Jin E, Yang J, Liang H, Zhao Y, Feng X, Narita A, Müllen K. Multilayer stabilization for fabricating high-loading single-atom catalysts. Nat Commun. 2020;11(1):5892. https://doi.org/10.1038/s41467-020-19599-8.
[68] Huang S, Qiao Z, Sun P, Qiao K, Pei K, Yang L, Xu H, Wang S, Huang Y, Yan Y, Cao D. The strain induced synergistic catalysis of FeN_4 and MnN_3 dual-site catalysts for oxygen reduction in proton-/anion-exchange membrane fuel cells. Appl Catal B. 2022;317:121770. https://doi.org/10.1016/j.apcatb.2022.121770.
[69] Pang Y, Su C, Xu L, Shao Z. When nitrogen reduction meets single-atom catalysts. Prog Mater Sci. 2023;132:101044. https://doi.org/10.1016/j.pmatsci.2022.101044.
[70] Iqbal MS, Yao Z, Ruan Y, Iftikhar R, Hao L, Robertson AW, Imran SM, Sun Z. Single-atom catalysts for electrochemical N_2 reduction to NH_3. Rare Met. 2023;42(4):1075. https://doi.org/10.1007/s12598-022-02215-7.
[71] Zou H, Rong W, Wei S, Ji Y, Duan L. Regulating kinetics and thermodynamics of electrochemical nitrogen reduction with metal single-atom catalysts in a pressurized electrolyser. PNAS. 2020;117(47):29462. https://doi.org/10.1073/pnas.201510811.
[72] Zang W, Yang T, Zou H, Xi S, Zhang H, Liu X, Kou Z, Du Y, Feng YP, Shen L, Duan L, Wang J, Pennycook SJ. Copper single atoms anchored in porous nitrogen-doped carbon as efficient pH-universal catalysts for the nitrogen reduction reaction. ACS Catal. 2019;9(11):10166. https://doi.org/10.1021/acscatal.9b02944.
[73] Liu Y, Fan X, Bian W, Yang Y, Huang P, Hofer WA, Huang H, Lin H, Li Y, Lee S. High-loading Fe_1 sites on vanadium disulfides: a scalable and non-defect-stabilized single atom catalyst for electrochemical nitrogen reduction. J Mater Chem A. 2022;10(39):21142. https://doi.org/10.1039/D2TA03994J.
[74] Li H, Chang SH, Zhang MM. Research progress on properties tuning and products of Cu–based catalyst in electrocatalytic CO2 reduction. Copper Engineering, 2023(6):38. https://doi.org/10.3969/j.issn.1009–3842.2023.06.005.
[75] Wang J, Zheng X, Wang G, Cao Y, Ding W, Zhang J, Wu H, Ding J, Hu H, Han X, Ma T, Deng Y, Hu W. Defective bimetallic selenides for selective CO_2 electroreduction to CO. Adv Mater. 2022;34(3):2106354. https://doi.org/10.1002/adma.202106354.
[76] Luo W, Xie W, Mutschler R, Oveisi E, De Gregorio GL, Buonsanti R, Züttel A. Selective and stable electroreduction of CO_2 to CO at the copper/indium interface. ACS Catal. 2018;8(7):6571. https://doi.org/10.1021/acscatal.7b04457.
[77] Zhan LS, Wang YC, Liu MJ, Zhao X, Wu J, Xiong X, Lei YP. Hydropathy modulation on Bi2S3 for enhanced electrocatalytic CO2 reduction. Rare Met. 2023;42(3):806. https://doi.org/10.1007/s12598-022-02212-whttps://doi.org/10.1007/s12598-022-02212-w. .
[78] Zhao Z, Zheng K, Huang N, Zhu H, Huang J, Liao P, Chen X. A Cu (111) @metal-organic framework as a tandem catalyst for highly selective CO_2 electroreduction to C_2H_4. Chem Commun. 2021;57:12764. https://doi.org/10.1039/D1CC05376K.
[79] Chen J, Wang T, Li Z, Yang B, Zhang Q, Lei L, Feng P, Hou Y. Recent progress and perspective of electrochemical CO_2 reduction towards C_2–C_5 products over non-precious metal heterogeneous electrocatalysts. Nano Res. 2021;14(9):3188. https://doi.org/10.1007/s12274-021-3335-x.
[80] Qu G, Wei K, Pan K, Qin J, Lv J, Li J, Ning P. Emerging materials for electrochemical CO_2 reduction: progress and optimization strategies of carbon-based single-atom catalysts. Nanoscale. 2023;15(8):3666. https://doi.org/10.1039/D2NR06190B.
[81] Li L, Shi YX, Hou M, Zhang ZC. Research progress of copper-based materials for electrocatalytic CO2 reduction reaction. Chin J Rare Met. 2022;46(6):681. https://doi.org/ 10.13373/j.cnki.cjrm.XY21120017.
[82] Yang H, Shang L, Zhang Q, Shi R, Waterhouse GIN, Gu L, Zhang T. A universal ligand mediated method for large scale synthesis of transition metal single atom catalysts. Nat Commun. 2019;10(1):4585. https://doi.org/10.1038/s41467-019-12510-0.
[83] Liu X, Liao L, Xia G, Yu F, Zhang G, Shu M, Wang H. An accurate "metal pre-buried" strategy for constructing Ni-N_2C_2 single-atom sites with high metal loadings toward electrocatalytic CO_2 reduction. J Mater Chem A. 2022;10(47):25047. https://doi.org/10.1039/D2TA07135E.
[84] Li M, Wang H, Luo W, Sherrell PC, Chen J, Yang J. Heterogeneous single-atom catalysts for electrochemical CO_2 reduction reaction. Adv Mater. 2020;32(34):2001848. https://doi.org/10.1002/adma.202001848.
[85] Karapinar D, Huan NT, Ranjbar Sahraie N, Li J, Wakerley D, Touati N, Zanna S, Taverna D, Galvão Tizei LH, Zitolo A, Jaouen F, Mougel V, Fontecave M. Electroreduction of CO_2 on single-site copper-nitrogen-doped carbon material: selective formation of ethanol and reversible restructuration of the metal sites. Angew Chem Int Ed. 2019;58(42):15098. https://doi.org/10.1002/anie.201907994.
[86] Zhao T, Wu YH, Song ZR, Wang X, Yin RL, Xu H, Cui H, Cao XH, Gao JK. MOF-derived nitrogen-doped iron-nickel oxide carbon nanotubes as efficient oxygen electrocatalyst for long-life rechargeable zinc-air batteries. Rare Met. 2023;42(10):3326. https://doi.org/10.1007/s12598-023-02415-9.
[87] Wu J, Zhou H, Li Q, Chen M, Wan J, Zhang N, Xiong L, Li S, Xia BY, Feng G, Liu M, Huang L. Densely populated isolated single Co-N site for efficient oxygen electrocatalysis. Adv Energy Mater. 2019;9(22):1900149. https://doi.org/10.1002/aenm.201900149.
[88] Jia C, Qin H, Zhen C, Zhu H, Yang Y, Han A, Wang L, Liu G, Cheng H. Ir single atoms modified $Ni(OH)_2$ nanosheets on hierarchical porous nickel foam for efficient oxygen evolution. Nano Res. 2022;15(12):10014. https://doi.org/10.1007/s12274-022-4501-5.
[89] Zhang L, Meng Q, Zheng R, Wang L, Xing W, Cai W, Xiao M. Microenvironment regulation of M-N-C single-atom catalysts towards oxygen reduction reaction. Nano Res. 2023;16(4):4468. https://doi.org/10.1007/s12274-023-5457-9.
[90] Shi Y, Zhou Y, Lou Y, Chen Z, Xiong H, Zhu Y. Homogeneity of supported single-atom active sites boosting the selective catalytic transformations. Adv Sci. 2022;9(24):2201520. https://doi.org/10.1002/advs.202201520.
[91] Yu B, Cheng L, Dai S, Jiang Y, Yang B, Li H, Zhao Y, Xu J, Zhang Y, Pan C, Cao XM, Zhu Y, Lou Y. Silver and copper dual single atoms boosting direct oxidation of methane to methanol via synergistic catalysis. Adv Sci. 2023;10(26):2302143. https://doi.org/10.1002/advs.202302143.
[92] Zeng M, Cheng L, Gu Q, Yang B, Yu B, Xu J, Zhang Y, Pan C, Cao X, Lou Y, Zhu Y. ZSM-5-confined Cr_1-O_4 active sites boost methane direct oxidation to C1 oxygenates under mild conditions. EES Catalysis. 2023;1(2):153. https://doi.org/10.1039/D2EY00080F.
[93] Jin H, Zhou K, Zhang R, Cui H, Yu Y, Cui P, Song W, Cao C. Regulating the electronic structure through charge

redistribution in dense single-atom catalysts for enhanced alkene epoxidation. Nat Commun. 2023;14(1):2494. https://doi.org/10.1038/s41467-023-38310-1.
[94] Zhang L, Zhou M, Wang A, Zhang T. Selective hydrogenation over supported metal catalysts: from nanoparticles to single atoms. Chem Rev. 2020;120(2):683. https://doi.org/10.1021/acs.chemrev.9b00230.
[95] Li S, Yue G, Li H, Liu J, Hou L, Wang N, Cao C, Cui Z, Zhao Y. Pd single atom stabilized on multiscale porous hollow carbon fibers for phenylacetylene semi-hydrogenation reaction. Chem Eng J. 2023;454(1):140031. https://doi.org/10.1016/j.cej.2022.140031.
[96] Kudo A, Miseki Y. Heterogeneous photocatalyst materials for water splitting. Chem Soc Rev. 2009;38(1):253. https://doi.org/10.1039/B800489G.
[97] Solakidou M, Giannakas A, Georgiou Y, Boukos N, Louloudi M, Deligiannakis Y. Efficient photocatalytic water-splitting performance by ternary CdS/Pt-N-TiO_2 and CdS/Pt-N, F-TiO_2: interplay between CdS photo corrosion and TiO_2-dopping. Appl Catal B. 2019;254(5):194. https://doi.org/10.1016/j.apcatb.2019.04.091.
[98] Mateo D, García-Mulero A, Albero J, García H. N-doped defective graphene decorated by strontium titanate as efficient photocatalyst for overall water splitting. Appl Catal B. 2019;252(5):111. https://doi.org/10.1016/j.apcatb.2019.04.011.
[99] Yan X, Liu D, Cao H, Hou F, Liang J, Dou SX. Nitrogen reduction to ammonia on atomic-scale active sites under mild conditions. Small Methods. 2019;3(9):1800501. https://doi.org/10.1002/smtd.201800501.
[100] Riyaz M, Goel N. Single-atom catalysis using chromium embedded in divacant graphene for conversion of dinitrogen to ammonia. ChemPhysChem. 2019;20(15):1954. https://doi.org/10.1002/cphc.201900519.
[101] Liu H, Cheng M, Liu Y, Wang J, Zhang G, Li L, Du L, Wang G, Yang S, Wang X. Single atoms meet metal-organic frameworks: collaborative efforts for efficient photocatalysis. Energ Environ Sci. 2022;15(9):3722. https://doi.org/10.1039/D2EE01037B.
[102] Qin S, Will J, Kim H, Denisov N, Carl S, Spiecker E, Schmuki P. Single atoms in photocatalysis: low loading is good enough. ACS Energy Lett. 2023;8(2):1209. https://doi.org/10.1021/acsenergylett.2c02801.
[103] Dou S, Dong CL, Hu Z, Huang YC, Chen JL, Tao L, Yan D, Chen D, Shen S, Chou S, Wang S. Atomic-scale CoO_x species in metal-organic frameworks for oxygen evolution reaction. Adv Funct Mater. 2017;27(36):1702546. https://doi.org/10.1002/adfm.201702546.
[104] Chen W, Pei J, He C, Wan J, Ren H, Wang Y, Dong J, Wu K, Cheong W, Mao J, Zheng X, Yan W, Zhuang Z, Chen C, Peng Q, Wang D, Li Y. Single tungsten atoms supported on MOF-derived N-doped carbon for robust electrochemical hydrogen evolution. Adv Mater. 2018;30(30):1800396. https://doi.org/10.1002/adma.201800396.
[105] Fang X, Shang Q, Wang Y, Jiao L, Yao T, Li Y, Zhang Q, Luo Y, Jiang H. Single Pt atoms confined into a metal-organic framework for efficient photocatalysis. Adv Mater. 2018;30(7):1705112. https://doi.org/10.1002/adma.201705112.
[106] Ma M, Huang Z, Doronkin DE, Fa W, Rao Z, Zou Y, Wang R, Zhong Y, Cao Y, Zhang R, Zhou Y. Ultrahigh surface density of Co-N_2C single-atom-sites for boosting photocatalytic CO_2 reduction to methanol. Appl Catal B. 2022;300:120695. https://doi.org/10.1016/j.apcatb.2021.120695.
[107] Shi R, Tian C, Zhu X, Peng C, Mei B, He L, Du X, Jiang Z, Chen Y, Dai S. Achieving an exceptionally high loading of isolated cobalt single atoms on a porous carbon matrix for efficient visible-light-driven photocatalytic hydrogen production. Chem Sci. 2019;10(9):2585. https://doi.org/10.1039/C8SC05540H.
[108] Choi CH, Kim M, Kwon HC, Cho SJ, Yun S, Kim H, Mayrhofer KJJ, Kim H, Choi M. Tuning selectivity of electrochemical reactions by atomically dispersed platinum catalyst. Nat Commun. 2016;7(1):10922. https://doi.org/10.1038/ncomms10922.
[109] Jiao C, Xu Z, Shao J, Xia Y, Tseng J, Ren G, Zhang N, Liu P, Liu C, Li G, Chen S, Chen S, Wang HL. High-density atomic Fe-N_4/C in tubular, biomass-derived, nitrogen-rich porous carbon as air-electrodes for flexible Zn-air batteries. Adv Funct Mater. 2023;33(20):2213897. https://doi.org/10.1002/adfm.202213897.
[110] Jiang M, Wang F, Yang F, He H, Yang J, Zhang W, Luo J, Zhang J, Fu C. Rationalization on high-loading iron and cobalt dual metal single atoms and mechanistic insight into the oxygen reduction reaction. Nano Energy. 2022;93:106793. https://doi.org/10.1016/j.nanoen.2021.106793.
[111] Rao P, Wu D, Luo J, Li J, Deng P, Shen Y, Tian X. A plasma bombing strategy to synthesize high-loading single-atom catalysts for oxygen reduction reaction. Cell Rep Phys Sci. 2022;3(5):100880. https://doi.org/10.1016/j.xcrp.2022.100880.
[112] Zhao C, Dai X, Yao T, Chen W, Wang X, Wang J, Yang J, Wei S, Wu Y, Li Y. Ionic exchange of metal-organic frameworks to access single nickel sites for efficient electroreduction of CO_2. J Am Chem Soc. 2017;139(24):8078. https://doi.org/10.1021/jacs.7b02736.
[113] Wang Q, Huang X, Zhao ZL, Wang M, Xiang B, Li J, Feng Z, Xu H, Gu M. Ultrahigh-loading of Ir single atoms on NiO matrix to dramatically enhance oxygen evolution reaction. J Am Chem Soc. 2020;142(16):7425. https://doi.org/10.1021/jacs.9b12642.
[114] Wang N, Mei R, Lin X, Chen L, Yang T, Liu Q, Chen Z. Cascade anchoring strategy for fabricating high-loading Pt single atoms as bifunctional catalysts for electrocatalytic hydrogen evolution and oxygen reduction reactions. ACS Appl Mater Inter. 2023;15(24):29195. https://doi.org/10.1021/acsami.3c04602.
[115] Xu C, Wu J, Chen L, Gong Y, Mao B, Zhang J, Deng J, Mao M, Shi Y, Hou Z, Cao M, Li H, Zhou H, Huang Z, Kuang Y. Boric acid-assisted pyrolysis for high-loading single-atom catalysts to boost oxygen reduction reaction in Zn-air batteries. Energy Environ Mater. 2022. https://doi.org/10.1002/eem2.12569.
[116] Wang H, Li X, Jiang Y, Li M, Xiao Q, Zhao T, Yang S, Qi C, Qiu P, Yang J, Jiang Z, Luo W. A universal single-atom coating strategy based on tannic acid chemistry for multifunctional heterogeneous catalysis. Angew Chem Int Ed. 2022;61(14):e202114722. https://doi.org/10.1002/ange.202200465.
[117] Cao D, Zhang Z, Cui Y, Zhang R, Zhang L, Zeng J, Cheng D. One-step approach for constructing high-density single-atom catalysts toward overall water splitting at industrial current densities. Angew Chem Int Ed. 2023;62(9):e202214259. https://doi.org/10.1002/ange.202214259.
[118] Dong H, Zhao Z, Wu Z, Cheng C, Luo X, Li S, Ma T. Metal-oxo cluster mediated atomic Rh with high accessibility for efficient hydrogen evolution. Small. 2023;19(15):2207527. https://doi.org/10.1002/smll.202207527.